AD NUMBER: AD0841178

LIMITATION CHANGES

TO:

Approved for public release; distribution is unlimited.

FROM:

Distribution authorized to US Government Agencies and their Contractors; Export Control; 1 Jun 1968. Other requests shall be referred to Air Force Rocket Propulsion Laboratory, Edwards AFB, CA 93524.

AUTHORITY

AFRPL ltr dtd 27 Oct 1971

AFRPL-TR-68-120

COMBUSTION SPECIES SAMPLING FINAL REPORT

Jack Kuhrs

Thiokol Chemical Corporation
Reaction Motors Division

Technical Report AFRPL-TR-68-120

June 1968

Air Force Systems Command, United States Air Force
Research and Technology Division
Edwards, California
Air Force Rocket Propulsion Laboratory

SPECIAL NOTICE

When U. S. Government drawings, specifications, or other data are used for any purpose other than a definitely related Government procurement operation, the Government thereby incurs no responsibility nor any obligation whatsoever, and the fact that the Government may have formulated, furnished, or in any way supplied the said drawings, specifications, or other data, is not to be regarded by implication or otherwise, or in any manner licensing the holder or any other person or corporation, or conveying any rights or permission to manufacture, use, or sell any patented invention that may in any way be related thereto.

BLANK PAGE

AFRPL-TR-68-120

COMBUSTION SPECIES SAMPLING

Final Report

Jack Kahrs

T. F. SEAMANS
Section Chief
Combustion & Physics Research

C. J. GRELECKI
Manager
Research Operations

J. R. WISEMAN
Director
Research & Engineering

THIOKOL CHEMICAL CORPORATION
Reaction Motors Division
Denville, New Jersey

FOREWORD

This report summarizes the results obtained in a program to improve the current state of sampling combustion species from high pressure sources. One part of this program dealt with a unique laboratory combustor which provides a continuously moving location for extracting combustion gases. This movable combustion chamber was designed, fabricated and tested in the program. A second effort was concerned with gas sampling processes including the transport of combustion species to a mass spectrometer. Specifically, an existing probe in use at RPL was analyzed and gas behavior was described. These efforts were performed under Contract F04611-68-C-0007, "Combustion Species Sampling", during the period 1 August 1967 to 1 May 1968. The internal report number is RMD 5530-F.

The work was administered under the direction of Capt. William H. Summers/RPCL and Mr. Charles M. Richey/RPFTR, Rocket Propulsion Laboratory, Edwards Air Force Base. It was designated as BPSN No. 673850, Project No. 3850, Program Element No. 6.54.02.15.F.

Contributions to the program have been provided by a number of members of the RMD Engineering Services Group. Mr. S. J. Kurzeja, in particular, was helpful in performing the computer calculations. Discussions with Professor John B. Fenn, Professor of Applied Science and Chemistry, Yale University, concerning aspects of the rarefied gas dynamics analyses have been extremely valuable. The Project Leader of the program was Mr. T. F. Seamans.

This technical report has been reviewed and is approved.

W. H. EBELKE, Colonel, USAF
Chief, Propellant Division
Air Force Rocket Propellant Lab.

ABSTRACT

A combustion chamber for propellant studies was developed and molecular beam gas sampling systems were analyzed in this program. A unique laboratory combustor design permits gas sampling from any part of the chamber by axial movement of an extraction port while the engine operates at pressures up to 500 psia. Variable chamber volume is also possible during operation. Sealing of moving pistons is accomplished by metal piston rings and elastomeric o-rings. Hot firings of the combustor with chlorine pentafluoride and hydrazine were made to demonstrate the operation of all components. The most severe test was of sixty seconds duration at chamber pressure of 455 psia with adiabatic flame temperature in excess of 4000°K. Effective hardware cooling, movement of the sampling station during firing and good combustion performance were successfully demonstrated.

In another part of the program, an existing gas sampling probe was examined to determine its effectiveness in transferring combustion species to a mass spectrometer. A capillary quenching channel in the sampling probe cools combustion gases from 4000°K to 1200°K but allows all dissociated species (in the case of hydrazine/chlorine pentafluoride) to recombine. At the exit of this channel, an unconfined free jet forms a typical underexpanded exhaust plume and the combustion sample undergoes several successive cycles of expansion cooling, shock reheating and dilution by background gases. Skimmer locations and chamber pressures were examined for suitable molecular beam formation. Recommendations are given for the design of more effective sampling probes.

CONTENTS

		Page
1.	INTRODUCTION	1
2.	SUMMARY	3
3.	PHASE I-MOVABLE COMBUSTION CHAMBER DESIGN	5
	3.1 General Mechanical Operation	5
	3.2 Injector Design	11
	3.3 Heat Transfer Analyses	12
	3.4 Actuation Mechanism	16
4.	PHASE II-DEMONSTRATION TESTING PROGRAM	21
	4.1 Laboratory Test Setup	21
	4.2 Test Results	24
5.	PHASE III-CHARACTERISTICS OF THE RPL/ROCKETDYNE PROBE	29
	5.1 Introduction to the Present Probe Analysis	29
	5.2 Dynamics of Channel Flow	32
	5.3 Chemical Kinetics of Channel Flow	49
	5.4 Free Jet Expansion	55
	5.5 Rarefied Gas Phenomena	61
	5.6 Mass Spectrometer Considerations	64
6.	AREAS OF POSSIBLE PROBE IMPROVEMENT	67
	6.1 Variation of Cooling Channel Parameters	67
	6.2 Future Improvemements	72
7.	CONCLUSIONS AND RECOMMENDATIONS	73
8.	REFERENCES	75

ILLUSTRATIONS

Figure		Page
1	Photo-Reduced Drawing of Movable Combustion Chamber, Thiokol-RMD Drawing X315513	19
2	Exploded View Photograph of Movable Chamber for Combustion Species Sampling	7
3	Movable Combustion Chamber Test Setup	22
4	Close-up Photograph of Movable Combustion Chamber in Position for Firing	23
5	Post-Test Nozzle Throat Cross-Section	27
6	Injector Water Flow Calibrations	28
7	Block Diagram of Gas Sampling System Pumping Stations (Reference 8)	30
8	Schematic Diagram of Present Sampling Probe Attached to Combustion Chamber (Reference 8)	31
9	Sketch of Present RPL/Rocketdyne Gas Sampling Inlet	34
10	Three-Dimensional Heat Transfer Nodal Network	38
11	Probe Temperature Distributions - ClF_5/N_2H_4 at O/F = 2.70 and P_c = 500 psia	40
12	Probe Temperature Distributions - N_2O_4/N_2H_4 at O/F = 1.44 and P_c = 500 psia	41
13	Gas Temperature Variations with Channel Length ClF_5/N_2H_4 at O/F = 2.70 and P_c = 500 psia	45
14	Gas Pressure Variation with Channel Length ClF_5/N_2H_4 at O/F = 2.70 and P_c = 500 psia	46
15	Gas Temperature Variation with Channel Length N_2O_4/N_2H_4 at O/F = 1.44 and P_c = 500 psia	47
16	Gas Pressure Variation with Channel Length N_2O_4/N_2H_4 at O/F = 1.44 and P_c = 500 psia	48
17	Sketch of Free Jet Structure for Highly Underexpanded Flows (Reference 22)	57
18	Characteristic Solutions for Free Jet Expansions with γ = 1.4 (Reference 23)	58

ILLUSTRATIONS

Figure		Page
19	Schematic Diagram of Present Sampling Probe Attached to Combustion Chamber	62
20	Influence of Probe Flow Diameter on Outlet Gas Temperature	68
21	Influence of Probe Channel Length on Outlet Gas Temperature	69
22	Influence of Probe Channel Wall Temperature on Outlet Gas Temperature	70

TABLES

		Page
I	Movable Chamber Injector Specifications	12
II	Typical Heat Sink Material Properties	15
III	Summary of Demonstration Test Results	25
IV	Summary of Gas Parameters in Subsonic Flow Through a Constant Area Duct	35
V	Gas Concentrations and Properties Used in Chemical Analyses	37
VI	Equilibrium Composition of the Combustion Products of Chlorine Pentafluoride and Hydrazine at O/F = 3.1, 500 psia, 4080°K	50
VII	Assumed Concentrations of Species Entering Cooling Channel of Probe	52
VIII	Approximate Species Concentrations at Cooling Channel Entrance and Exit for a Range of ClF_5/N_2H_4 Mixture Ratios	56
IX	Summary of Some Alternate Approaches to Using the Present RPL/Rocketdyne Probe	71

ABBREVIATIONS AND SYMBOLS

A	area
c	specific heat
D	diameter, dimension
F	fuel weight
k	reaction rate constant
K	thermal conductivity, equilibrium constant
L	length
L*	characteristic length, chamber volume/throat area
M	chemical species, Mach number
O	oxidizer weight
p	pressure
R	universal gas constant
t	time
T	temperature
V	volume
w	mass flowrate
W	molecular weight
x	distance
Y	weight fraction
z	characteristic time
γ	ratio of specific heats
λ	mean free path
ν	coefficient for reactants or products
ρ	density
τ	characteristic time, reaction time

SUBSCRIPTS

a	ambient
c	convection, chamber
D	dissociation
f	fuel
h	hydraulic
M	Mach disk
n	node
o	oxidizer, stagnation, initial
p	pressure
r	radiation
R	recombination
s	static

BLANK PAGE

1. INTRODUCTION

Although there is much speculation, little is known of the combustion processes occurring within rocket engines or other similar high energy devices. Because of simultaneous fluid injection, atomization, vaporization, multiple chemical reaction paths, and a variety of possible local phenomena, the analytic description of events within a combustion chamber is extremely difficult. Consequently, experimental measurement of combustion phenomena becomes important in those cases where performance and reliability are critical or where an understanding of the basic processes is desired. Because of the fundamental value of the information obtained, gas extraction and sampling is a classical experimental technique receiving ever-increasing attention today in combustion research.

Sampling of gases from a combustion chamber and subsequent analysis by mass spectrometer can provide considerable insight into the chemistry of reaction mechanisms. In order to define the progress of a reaction, however, measurements must be obtained as a function of location in the reaction zone, hence the need for a moving sampling station. One portion of this program was the design of a movable combustion chamber to fill this need.

For valid gas analyses, the sample extraction system must effectively quench the high temperature reactants and transport the gases unchanged to the mass spectrometer. This facet of high pressure combustion gas sampling was also investigated.

In its entirety, Contract F04611-68-C-0007 consisted of three phases with the following objectives:

Phase I - Analysis and design of a combustion chamber with a sampling station whose axial location can be continuously varied during operation. The design was based on use of chlorine pentafluoride/hydrazine, although use of other propellants is feasible. The new combustor is interchangeable with fixed-sampling-port chambers presently operational at the A. F. Rocket Propulsion Laboratory.

Phase II - Fabrication and demonstration testing of the movable combustion chamber.

Phase III - Analytical investigation of the current Rocket Propulsion Laboratory (RPL) sampling probe to determine its effectiveness in transporting chamber species to a mass spectrometer.

This report summarizes the work performed and the conclusions reached in all phases.

2. SUMMARY

The objectives of the current program are (a) to develop a laboratory combustion chamber which traverses during operation relative to a fixed, side-mounted gas sampling/extraction system and (b) to evaluate analytically the effectiveness of an existing AFRPL gas sampling/extraction system. The combustion chamber was designed and fabricated. A demonstration testing program was conducted. The analysis of the existing gas sampling/extraction system reveals serious deficiencies in the design. Probe improvements are defined.

The combustion chamber was designed to provide movement of the gas extraction port with respect to the injector and exhaust nozzle during operation at 500 psi. Since the sampling port connects to large diameter piping, closely coupled vacuum pumping equipment and a mass spectrometer, the port remains fixed while the injector and exhaust nozzle translate within the cylindrical combustion chamber. An alternate mode of operation allows the exhaust nozzle also to be fixed to the main housing while only the injector is moved yielding an engine with varying chamber volume (L*) during operation.

Chamber diameter is 1.25 inches and exhaust nozzle throat diameter is 0.160 inches while chamber length can be varied from 0.5 to 3.0 inches yielding characteristic lengths from 37 to 189 inches. A combined hydraulic/pneumatic actuation system provides variable traversing speeds of the injector and exhaust nozzle ranging from one inch per minute to 2.5 inches per second. Sealing of the moving pistons is accomplished by a metal piston ring assembly backed by two elastomeric o-rings. The piston rings halt the flow of hot gases while the o-rings, located in cooled walls, provide a positive seal.

The injector, chamber barrel and exhaust nozzle are each separately cooled with water. Analyses have indicated that chamber operation with flame temperatures of 4000°K for durations up to 60 seconds is practical.

Injector design employed a uniform mixing criterion for chlorine pentafluoride and hydrazine. To provide maximum circumferential uniformity of chamber species, a single injector element of four oxidizer streams impinging on a single fuel stream is used. Large L/D inlet orifices assure fully developed turbulent flow and optimum propellant mixing.

The testing program successfully demonstrated operation of all components of the movable combustion chamber. A 60 second test at 455 psia indicated that the combustor design is adequate for its intended use.

The analytical investigation of the existing gas sampling system for transporting combustion species to a time-of-flight mass spectrometer contained several major elements. The location of the sample extraction port in the wall of the combustion chamber and the design of the probe entrance appear adequate to obtain a representative sample from the chamber.

Analysis of the cooling channel has shown that although gas temperature drops rapidly, the outlet pressure and temperature are still much higher than desirable for a sampling probe. A consequence of the cooling channel behavior in the case of ClF_5/N_2H_4 products is complete recombination of all free atoms existing in the combustion chamber. Gases at the exit of the cooling channel are therefore not representative of those existing in the chamber.

When the gases emerge from the channel, they expand in a free jet going through a familiar exhaust plume structure before entering the first skimmer. Gases drawn through the skimmer are consequently an unknown mixture of background and reacting sample species. The performance of the first probe chamber is considered one of the weakest aspects of the present probe.

The flow of gas through the first skimmer is choked and the mass flow is controlled by entrance conditions. Flow in the second probe chamber consists of a free jet expansion with an isentropic core which is intercepted by the second skimmer. This skimmer is properly located for molecular beam formation and preservation of the sample. Unfortunately, the sample may be considerably different at this point than its original chamber composition.

It appears that significant improvements in the sampling system are possible using the present pumping systems but a drastically revised arrangement of probe chambers.

3. PHASE I - MOVABLE COMBUSTION CHAMBER DESIGN

The Rocket Propulsion Laboratory at Edwards Air Force Base presently has a small water cooled combustor, a probe which extracts gas samples from the combustion chamber and a time-of-flight mass spectrometer for sample identification. Their system and studies represent a pioneering effort in obtaining data on high pressure combustion chamber phenomena. In order to obtain gas samples from all locations in the reaction vessel, an improved system is required which provides movement of the sampling station location during operation of the engine.

There are many possible approaches to obtaining relative motion between the combustion chamber and sampling port. However, since the gas extraction system has associated with it several vacuum diffusion pumps, cooled baffles and large diameter piping all coupled to the flight tube of a mass spectrometer, it is necessary that this large assembly remains stationery and that the combustion chamber moves with respect to this system and the remainder of the laboratory. We have accomplished this by providing a fixed cylindrical barrel (the body of the combustion chamber) within which can slide an injector and an exhaust nozzle. Each of the sliding components can be attached to an actuator which is controlled remotely.

The following sections discuss initially the design approach to the overall assembly, and secondly some of the features of individual components.

3.1 General Mechanical Operation

Long duration firings with high temperature propellants in a chamber with dynamic hot gas seals required careful study of all factors involved in combustion chamber design and fabrication. One aspect of the design effort is shown in Drawing X315513, photographically reduced for Figure 1. For convenience, this figure has been placed at the end of this section, page 19. Design of all components of the combustion chamber assembly has stressed simplicity and reliability. With the need for extended duration tests, water cooling is necessary and the simplicity sometimes possible with uncooled hardware was not possible in this case.

In the injector, the water cooling passages have been designed to be easily separable from the propellant passages. This feature will greatly enhance the flexibility of the combustion chamber in permitting use of

alternate injectors designed for other propellants. A minor sacrifice in design simplicity was necessary to obtain this feature since the injector is separate from the cooling jacket. As shown in Figure 1, the actuator, Part Number 6, is a commercially available system. It is extremely versatile and provides full movement of the injector and exhaust nozzle in any time period from 1 to more than 60 seconds. The actuation force is applied through a rod end bearing (PN 11) and locking pin (PN 10) which provide alignment and ease of disassembly.

In the assembly drawing, two sets of bolts are shown holding the exhaust tube to the chamber body (PN's 34 and 40). If a non-moving exhaust nozzle is desired, the bolts in the front view are used (PN 34), but not the others. This selection will result in variable L* operation when the injector is moved. On the other hand, when constant L*, movable sampling station operation is desired, the bolts shown in the top view (PN 40) fixing the exhaust tube to the traversing frame are used. The bolts shown in the front view of the exhaust tube are not used in this case.

The top view also shows the propellant valves which mount to the traversing frame and move with the injector. Flexible lines are used between rigidly mounted safety valves of the laboratory propellant system and the moving main valves. If the valves were not attached to the traversing frame, the injector dribble volume would have to be very large. Starting and stopping transients would be excessively long.

Attachment of the exhaust tube to the scrubber is through a standard flange, shown at the extreme right of Figure 2. Since the RPL scrubber is mounted on wheels, careful alignment is required to eliminate any radial loads on the chamber assembly.

The chamber pressure tap is located directly opposite the gas sampling port. The nickel liner of the chamber is restrained only at these two central locations to permit axial growth while heating. Piston ring grooves and material tolerances have been determined to be correct when the liner reaches its steady state operating temperature.

On the top of the stationary chamber in Figure 2 is shown the inlet section of the RPL gas sampling probe. The combustion chamber is fully compatible with the RPL mass spectrometer/sampling system.

Components which are available as catalog items and which were purchased are indicated on the assembly drawing. The most prominent of these is the Alkon actuator shown at the left of Figure 2. The Marotta fuel valve is shown at the bottom and the Control Components Inc. oxidizer valve is shown at the top of Figure 2.

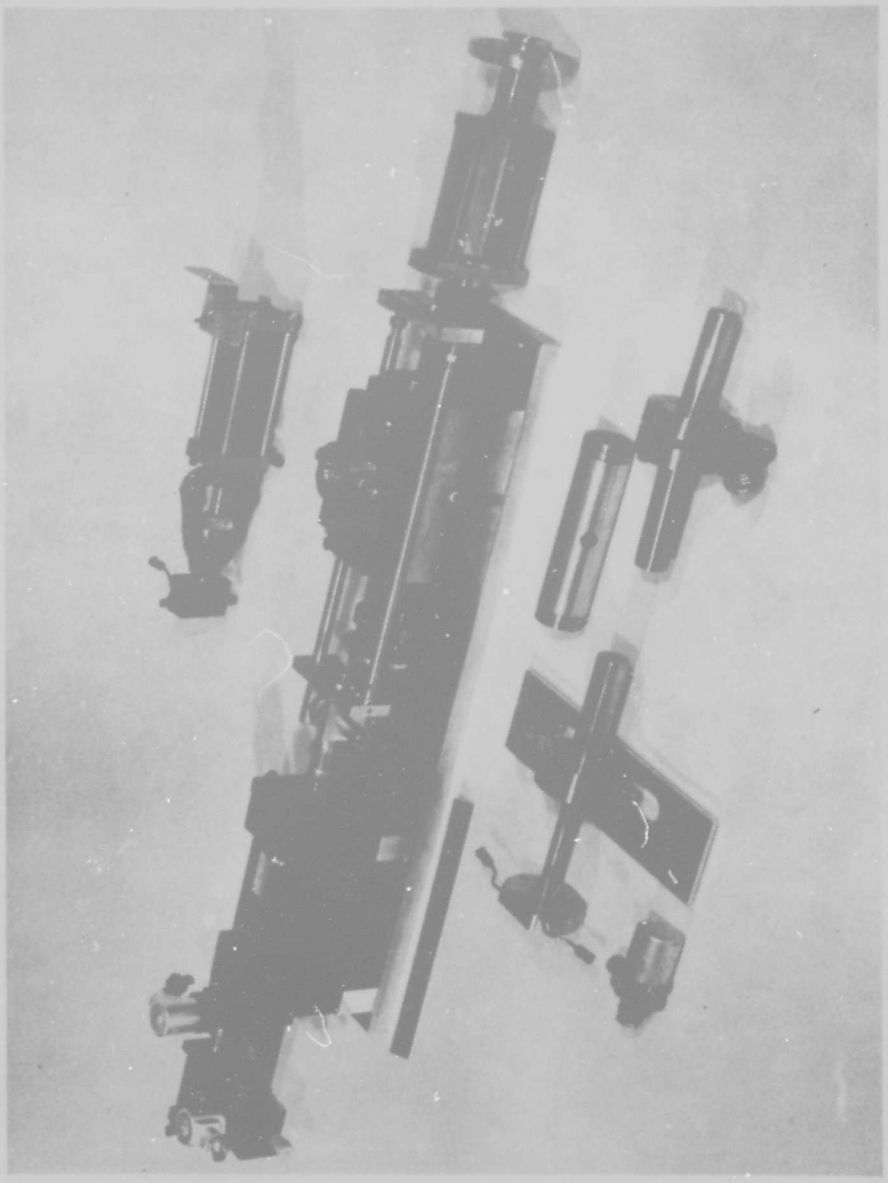

Figure 2
Exploded View Photograph of Movable Chamber For
Combustion Species Sampling

3.1.1 Hot Gas Seal Design

The approach to sealing the hot combustion gas during movement of the combustion chamber is of primary importance to reliable chamber operation. Many concepts were examined.

Details of the metal piston ring assembly (chosen for its advantages over other possibilities) are shown in the enlarged inserts in the center of Figure 1. A commercially available five-piece metal piston ring assembly is used for primary gas blockage and support of the moving piston. A split gland is used for each piston to simplify assembly and maintenance. Two elastomeric o-rings are used to back up each piston ring to provide a leak-tight seal. The o-rings are placed at a location which is sufficiently cooled for them to be effective.

A completely different approach consisting of a "Bellofram" flexible rolling diaphragm assembly would have provided a very low friction, leak-free seal. This type of unit would have to be custom fabricated and as a result would be much more costly than other seal arrangements. In addition, chamber pressures of 500 psi represent an upper limit for this type of device. This approach, therefore, was considered not completely satisfactory.

Other approaches that were briefly investigated were graphitic ring assemblies and welded metal bellows assemblies. The graphite requires extensive "running in" to seal properly and reliably and in addition oxidizes rapidly at high temperatures in ox-rich environments. Welded metal bellows would have to be custom fabricated and would be relatively expensive. However, they provide a positive seal where space is available for their use.

Elastomeric Material Selection

The estimated wall temperature at the location of the elastomeric o-rings providing the hot gas seal in the chosen design is considerably less than 400°F. In this case, both silicone rubber and "Viton A" are suitable o-ring materials. The specifications for silicone rubber state that continuous operation at 450°F with short duration exposure to 700°F is permissible. Similar specifications for the best high temperature Viton compound state that 400°F continuously or 600°F for short periods are satisfactory. In addition, Viton has shown itself serviceable in situations where temperatures have reached 900°F (for five minutes or less) becoming only slightly hardened.

For oscillating seals, one o-ring manufacturer recommends a durometer hardness of 80-90 in order to prevent chatter and to obtain smooth movement. A higher hardness will also reduce the tendency of the o-ring to be forced (extruded) into the narrow gap beyond the groove. Another manufacturer recommends 85 durometer as a top limit for leak-free dynamic applications with compounds of 70-80 Shore A durometer representing a most suitable compromise for average conditions.

O-ring materials suitable for this application are:

	Parker Specification
Silicone	
70 durometer	S451-7
80 durometer	S467-8
Viton	
72 durometer	77-545
88 durometer	V274-9

The Viton compound 77-545 is standard, readily available and meets all requirements. It has been specified on the detail drawings although the other compounds appear to be equally suitable should future usage dictate a change.

3.1.2 Chamber Volume

The size and shape of the combustion chamber which has been selected represents a number of compromises to meet slightly divergent aims. First, a chamber L* (combustor volume/nozzle throat area) which could be made as large as 200 inches was desired for some studies to provide a sufficiently long residence time to guarantee reaction completion. The minimum L* was determined partly by the probe tip which extends into the chamber and restricts complete freedom of movement of the pistons. Layouts of the injector with its propellant passages and coolant water passages indicated the desirability of large chamber diameters. In addition, if the diameter were too small, the chamber would have to be excessively long to sweep out the required volume.

As designed, the combustion chamber has the listed characteristics. Selection of thrust level and chamber pressure resulted in a specified throat area of .020 in^2.

Chamber diameter	1.25 inches
Maximum chamber length	3.0 inches
Maximum L*	189 inches
Minimum length	0.5 inches
Minimum L*	37 inches
Maximum effective sampling port travel	2.5 inches

3.1.3 Materials and Manufacturing

In all cases, the choice of materials was made in light of thermal and structural requirements and chemical compatibility.

Because of the desired injector orifice characteristics (high L/D) and because of the low flowrates, long, very small diameter holes are required. These passages can be made either by use of hypodermic tubing or by modern hole forming techniques. The hypodermic tubing is most effective in a 1-on-1 injector where there is no manifolding required. The four oxidizer passages in the present design would require a manifold which would be difficult to fabricate with small tubing. We chose, therefore, to form the holes in a solid piece of nickel through use of an Electrical Discharge Machine (EDM). This device, which has become a standard tool in many shops, advances a cooled electrode of the proper diameter into the material creating local overheating and surface failure, thereby forming a hole. The hole sizes specified for the injector are well within the state of the art.

Joining of several combinations of materials of critical dimensions was done by Electron Beam (EB) Welding where more conventional techniques were not completely suitable. In this method, a very localized intense heating provides material flowing from both surfaces which bonds upon cooling. The localized heating prevents the distortion which might otherwise occur with other types of welding.

There were no difficult assemblies in the Movable Combustion Chamber for which unusual fabrication problems resulted. A comprehensive tabulation of compatibility of chlorine trifluoride and MHF-3 with materials of construction is given in Reference 1. Also in that reference are manufacturers' data for components specified for the movable combustion chamber.

3.2 Injector Design

The injector of a liquid propellant rocket engine plays a fundamental role in the success of the overall design. Although combustion performance is most directly linked with the injector, other important parameters such as heat rejection rate and combustion stability also depend on injector design. Since we are concerned with a wide variety of propellants and since thrust levels cover a wide range (although not in this program), no universal approach to propellant injection is possible. Each case must be considered with its unique requirements.

It has been shown rather conclusively that the attainment of maximum performance follows as a result of a controlled mass and mixture ratio distribution across the injector face. Overall propellant mixture ratio, determined by inlet flow rate, is chosen to provide a specified bulk temperature of the combustion products, generally close to the maximum attainable. The reaction between propellants, however, takes place on the molecular level, hopefully at the same mixture ratio. It is apparent then that on any macroscopic scale at any location in the chamber it is desirable to provide appropriate proportions of reactants and/or products. One popular approach to determining whether an injector does provide a uniform mixture ratio is through the use of non-reactive, immiscible simulant fluids. The spray formed by the injector is collected in small individual tubes and a direct measure of local mixture ratio is obtained. Tests such as these have permitted correlation of injection stream properties to define the requirements for optimum mixing.

For an impinging stream injector of the 4-on-1 type, this correlation was formulated by Elverum and Morey (2). Their results indicate that optimum mixing for streams with total included angle of 60° is obtained when the relation

$$\left(\frac{w_1}{w_2}\right)^2 \frac{\rho_2}{\rho_1} \left(\frac{A_2}{4A_1}\right)^{1.25} = 2.90$$

is met. Since we are not primarily concerned with the fundamentals of injector design in this effort, it will suffice to say that the above relation was used to determine the injector area ratio. Subscript 1 refers to the four outer streams while subscript 2 represents the central stream. It can also be seen that once an area ratio has been selected for optimum mixing with a particular propellant combination (ρ_1/ρ_2), at a particular mixture ratio

(w_1/w_2), any other value of $(w_1/w_2)^2 (\rho_2/\rho_1)$ will not give the best performance. Here we assume that optimum mixing and best performance are synonymous.

Correlations for other types of impinging stream injectors have been summarized by Riebling (3).

The results of these correlations are strictly valid only for streams having symmetrical, uniform velocity profiles. This requirement can be met most easily by providing fully developed turbulent flow in the injector passages. The necessary L/D varies from approximately twenty, when a turbulence inducing entrance section is employed, to approximately fifty without it. These requirements are met in our design. Injector specifications are given in Table I for optimum mixing of chlorine pentafluoride/hydrazine.

Table I

Movable Chamber Injector Specifications

Central fuel hole diameter	.018 - .019
L/D	50
w_f (hydrazine)	.012 lb/sec
Δ_p	94 psi
Reynolds number	15,300
Diameter of each of four oxidizer holes	.012 - .013
L/D	20
w_o (chlorine pentafluoride)	.037 lb/sec
Δ_p	62 psi
Reynolds number	36,700

The discussion of the design of the combustion chamber noted that the injection section can be taken out of its cooling jacket. To test different propellant combinations, only additional injector orifice sections need be fabricated since the cooling jacket will be common to all.

3.3 Heat Transfer Analyses

To assure reliable, long duration testing capability and to minimize any chamber development programs after fabrication, several extensive heat transfer analyses were conducted. It is recognized that many complex interrelated phenomena affect the heat transfer to the walls of a rocket engine.

Among these are radiation, turbulence, non-uniform or secondary flows and chemical reactions. Correlations relating heat flux to mass flowrate, geometry and fluid properties are surprisingly successful in view of the complexities. There is a variety of approaches available in the literature for predicting combustion chamber heat flux and where a margin of safety is available, all are generally comparable.

Because of the necessity for movement of injector and exhaust nozzle, each of these components has its own coolant supply and return ports. The combustion chamber barrel also has its own coolant system. The coolant water supply characteristics were partially dictated by an existing water pump in the AFRPL test stand. This pump is manufactured by Aldrich having a maximum flow rate of about 7.2 lb/sec at 540 psig.

In general, it is desirable to pressurize the coolant to levels greater than combustion chamber pressures so that in the event of a minor wall failure, the flow of coolant will be into the chamber. If this occurs, the probability is high that detection, test termination and subsequent repair will be successful. Since chamber pressure will approach 500 psia a coolant supply pressure of approximately 700 psia is desirable. The Aldrich Pump available at RPL, however, has a maximum outlet pressure of 540 psig and the desired pressure difference will not be available with the existing pump. If desired, the pump can easily be modified to provide outlet pressures up to 875 psi.* The present pressure deficiency should not impair the effectiveness of the heat transfer design under normal combustion chamber operation.

Basic Design Conditions

Since the movable combustion chamber is intended for use in a variety of laboratory studies, representative design parameters were selected for the most severe conditions to be encountered. The maximum flame temperature of commonly used propellants results from ClF_5/N_2H_4, therefore, the properties of this combination were generally employed in the thermal analyses.

Theoretical flame temperature of ClF_5/N_2H_4 is above 4000°K for a range of mixture ratios. The throat area of the exhaust nozzle is 0.02 square inches, and the chamber diameter is 1.25 inches. Both the chamber and the nozzle/exhaust tube are cooled by water flowing through an annulus. The nozzle and exhaust tube are an integral unit and are therefore cooled together, while the chamber has its own coolant supply. The injector is also cooled by water flowing through a coolant ring. Where possible,

* Replacement parts include a new plunger, packing and bushings at a cost of approximately $800.

nickel has been selected as the material of construction exposed to exhaust gases because of its erosion resistance. A basic design goal is to keep the steady state temperature of the hot surfaces at, or below, 800°F, however, the thermal conductivity of nickel is too low to maintain this temperature in the throat section. For this reason, copper is used in the throat because it combines a much higher thermal conductivity with good erosion resistance.

Detailed results of the analyses of each section are given below. The configuration of each component can be seen in the drawing of Figure 1.

Injector

The injector was analyzed on a one-dimensional basis, assuming a heat transfer coefficient equal to the chamber heat transfer coefficient. The injector was made of nickel and cooled by a water jacket extending the full length of the injector. The coolant water flowrate required to keep the face of the injector at 800°F during steady state operation is 1.4 lb/sec.

Chamber

The chamber wall is constructed of nickel, 1/16" thick and cooled by water flowing in a 1/8" annulus. For a water mass flow rate of 0.5 lb/sec, the heat rejection is 0.57 BTU per inch of chamber length. The steady state gas side wall temperature is 510°F.

Nozzle

The nozzle is made of OFHC copper, 1/16" thick and cooled by water flowing in a 1/16" annulus. The wall temperature at the throat is 800°F during steady state operation. The total heat rejection upstream of the throat, but downstream of the chamber is 2.59 BTU/sec. Water requirements are 2.2 lbs/sec.

Exhaust Extension

The exhaust extension is made of 1/16" thick nickel, with water flowing through a 1/8" annulus. The steady state operating temperature is 236°F. The coolant water used is the same as that used for cooling the throat.

Heat Sink Combustion Chambers

Because of the complexity of the water cooled components and the possibility that many tests could be run for short durations, heat sink combustion chambers were considered. The materials examined were copper, beryllium and ZTB graphite. Pertinent properties are given in Table II.

Table II

Typical Heat Sink Material Properties

	K (Btu/hr-ft-°F)	c_p (Btu/lb-°F)	ρ (lb/ft³)	$K c_p \rho$	Allowable Surface Temp(°F)
Copper	224	.098	558	12100	800
Beryllium	75	.6	116	5230	800
ZTB Graphite	127.1	.5	123.5	7850	3500

Generally speaking, the best heat sink is copper, but since its allowable surface temperature for this application is low, graphite may be more favorable. Grade ZTB graphite was selected due to its high density and thermal conductivity. Its allowable surface temperature is approximate, but believed to be conservative for the present environment. Beryllium is a useful heat sink due to its high specific heat. However, its low density, which is useful in weight limited applications, is not a desirable property for the present volume limited application.

Based on the parameters given above, a one dimensional, transient heat conduction calculation using Hill's method (4) was made for each of the heat sink materials, assuming an insulated rear surface.

Beryllium performed the worst, having a useful life of about 0.1 seconds. Copper has a useful life of about 0.4 seconds. Graphite can be used for about 4 seconds before its surface temperature increases above 3500°F. However, the rear surface of the graphite will rise to over 1000°F in about 1-1/2 seconds and its useful life is only about 1 second. Therefore a more complicated hot gas seal design is required to accommodate the high temperature insert.

Heat sink chamber design does not appear to be satisfactory except for much lower temperature propellant systems and no further consideration was given to this approach.

The effects of heat losses on a small water cooled engine were analyzed and found to be negligible. Details of this analysis are given in Reference 1.

3.4 Actuation Mechanism

The overall approach of moving the injector and exhaust nozzle simultaneously or separately within a fixed cylindrical barrel has been described previously. The reason for this approach can be traced to the combined bulk of the sampling probe which is a part of the cylindrical chamber wall and the associated vacuum pumping equipment.

For traversing the entire combustion chamber past the fixed sampling port, AFRPL requested total travel times ranging from 1 second to 60 seconds. Actuation mechanisms were examined, therefore, with a goal of 60:1 speed variation along with the usual aims of reliability, economy and practicality.

Electric motors and ball screw actuators of several different types were examined. Gearmotors with mechanically variable gear ratios are available but cover only a 10:1 speed ratio. Variable speed motors with solid state speed controls are available with linear actuators. However, they are both expensive and generally too small for this application. Gearmotors having sufficient power with electronic speed controls are available for speed ranges of 30:1. However, when combined with the required ball screw actuator, the cost becomes very high.

Hydraulic actuation systems, on the other hand, are much more economical and provide greater capability for speed variation. The system which has been selected for this application is shown in Figures 1 and 2 and has the following features. A power cylinder with 2.5 inch bore provides the actuation force. Compressed air or nitrogen is bled into this cylinder from lab or bottled supplies. The maximum pressure, required when the chamber nozzle is held stationary and only the injector is moved, is approximately 200 psig. The actuation unit and controls are factory preassembled by Alkon Products Corporation. The hydraulic unit has a double "Stop Feed" option consisting of an electric valve and a metering orifice enabling the Feed Control to be stopped at any point in the stroke, dwell there, and restart. Two valves are used to provide this option in either direction of travel.

Each valve allows the Feed Control to operate until the valve is energized whereupon it completely blocks off the oil flow and stops movement. Each Stop Feed valve has an adjustable metering screw so that regulated feed can be obtained as required. The feed control system can provide the 2.5 inch travel of the injector and exhaust nozzle in a fraction of a second or in approximately 2.5 minutes by means of a simple micrometer valve setting.

The extreme versatility and reliability of this system seems outstanding.

To summarize actuator capability:

Minimum time to traverse 2.5 inches, $\leq$ 1 second
Maximum velocity, $>$ .21 feet/second
Maximum gas flowrate for power cylinder, $\sim$ .43 cfm @ 200 psig
Minimum velocity, $<$ .0035 feet/second

The minimum and maximum velocities noted above correspond to a full 2.5 inch traverse in 60 seconds or 1 second, respectively.

⚠ ACTUATOR CONSISTS OF
1. POWER CYLINDER MODEL D-32-1-3½"-4"-STYLE 2
2. FEED CONTROL UNIT (W/STOPS, ELECTRIC VALVES & CALIBRATED KNOBS) NO. D8323-4"
3. TANDEM COUPLING KIT NO 8938-3½
ALKON PRODUCTS CORP
WAYNE, NEW JERSEY CODE IDENT 96556

⚠ MODEL MV100WD VALVE
MAROTTA VALVE CORP
BOONTON, NEW JERSEY CODE IDENT 99657

⚠ CCI NO CM 60 06 P VALVE
CONTROL COMPONENTS INC
LOS ALAMITOS, CALIF. CODE IDENT 19662

⚠ BLDC 12-20 BALL LOK PIN
AVDEL INC.
BURBANK, CALIF. CODE IDENT 84256

⚠ HFF-12C ROD END
THE HEIM UNIVERSAL CORP
FAIRFIELD, CONN CODE IDENT 73134

⚠ TYPE MX-1 PART NO SP4246-128
COOK AIRTOMIC DIV
DOVER CORP
LOUISVILLE KY CODE IDENT 71687

⚠ MODEL 108 4.00" TRAVEL POTENTIOMETER
THREADED SHAFT #10-32 NF-3 X ¾ LONG
BOURNS LABORATORIES INC.
RIVERSIDE, CALIF. CODE IDENT 80294

⚠ MAKE FROM MS 16998-34
MACHINE LENGTH TO 1.650

⚠ GOV'T FURNISHED EQUIPMENT

⚠ ALIGN SLOTS IN ITEM 16 WITH PORTS IN ITEM 14

⚠ MACHINE ITEM 25 TO ALIGN CENTER LINE OF ACTUATOR TO PROVIDE SMOOTH OPERATION OF COMPLETE UNIT

⚠ CLEAN PER RMD SPEC 7424
PROPELLANT FLOW PASSAGE ONLY

1	A5	71	X427897-01	-	SLEEVE
1	A5	70	MS9021-014	-	"O"-RING
1	B8	69	X315513-10	A	TUBE
1	B8	68	X315513-07	A	TUBE
4	B8	67	AN525B9-20	-	SLEEVE
4	B8	66	AN819-9C	-	NUT
1	B5	65	MS9021-30	-	"O"-RING
2	D6	64	AN345C10	-	NUT
1	B8	63	11-13056-128	-	"O" RING
2	C4	62	AN505-6-5	-	SCREW
2	C5	61	AN960PD10	-	WASHER
1	B8	60	11-10025-9	-	"O" RING
2	B6	59	11-10036-133	-	"O" RING
2	B6	58	11-10036-129	-	"O" RING
4	B5	57	11-10034-024	-	O RING
2	A9	56	11-10034-018	-	"O" RING
4	B8 A7	55	MS29512-68	-	"O" RING
1	B6	54	MS9021-029	-	"O" RING
2	B5 B7	53	MS9021-32	-	"O" RING
1	A4	52	MS20827-25	-	ELBOW
1	B8	51	11-10026-4	-	O RING
1	B8	50	AN929-45	-	REDUCER
2	C5	49	MS21919DG6	-	CLAMP
1	B8	48	AN919-15	-	REDUCER
4	B5 A7	47	AN815-8C	-	UNION
2	B7	46	MS20365-428	-	NUT
4	B8 A8	45	MS20365-832	-	NUT
2	D6	44	MS16996-9	-	BOLT
2	D5	43	AN505-4-4	-	SCREW
2	B7	42	MS16996-49	-	BOLT
2	C5	41	MS16996-21	-	BOLT
2	D5	40	MS16995-70	-	BOLT
2	D7	39	MS16995-72	-	BOLT
2	B8	38	MS16996-16	-	BOLT
6	A8 A6	37	MS16996-11	-	BOLT
8	A7 A6	36	MS16996-25	-	BOLT
4	B5	35	MS16996-22	-	BOLT
2	B5	34	MS16995-71	-	BOLT
4	A4	33	MS16996-88	-	BOLT
1	B6	32	X66F18257	-	BLEEDER ⚠
4	C8	31	MS16997-47	-	BOLT
1	A9	30	X427894-01	-	SPACER
2	C7	29	X427898-01	-	SPACER
1	B7	28	X427894-01	-	SPACER
1	C4	27	X427897-01	-	BRACKET
4	D6	26	X315513-08	M/C	BOLT ⚠
1	A4	25	X427895-01	-	GASKET
1	A4	24	X427889-01	-	SCREW
2	A9	23	X427893-01	-	SPACER
1	D5	22	X427892-01	-	BRACKET
1	C5	21	X427891-01	-	BRACKET
1	A7	20	X427885-01	-	BASE
1	C7	19	X427884-01	-	PLATE
1	B6	18	X427888-01	-	FLANGE
1	B5	17	X427887-01	-	FLANGE
1	B6	16	X427896-01	-	SPACER
1	B6	15	X427884-01	-	SLEEVE
1	B4	14	X427890-01	-	BODY
1	D6	13	X315513-07	M/C	POTENTIOMETER ⚠
2	B6	12	X315513-06	M/C	SEAL-PISTON ⚠
1	D7	11	X315513-05	M/C	ROD END ⚠
1	D7	10	X315513-04	M/C	PIN ⚠
1	B5	9	X315515-100	-	EXHAUST TUBE
1	B6	8	X315513-03	M/C	OXIDIZER VALVE ⚠ ⚠
1	D8	7	X315513-02	M/C	FUEL VALVE ⚠
1	C7	6	X315513-01	M/C	ACTUATOR ⚠
1	B5	5	X315514-100	-	HOUSING
1	D5	4	X315516-100	-	FRAME
1	B6	3	X315511-100	-	JACKET
1	B7	2	X315510-100	-	INJECTOR
1	B5	1	X315512-100	-	NOZZLE

		Thiokol CHEMICAL CORPORATION REACTION MOTORS DIVISION	
		MOVABLE COMBUSTION CHAMBER	
		J 83323	X315513

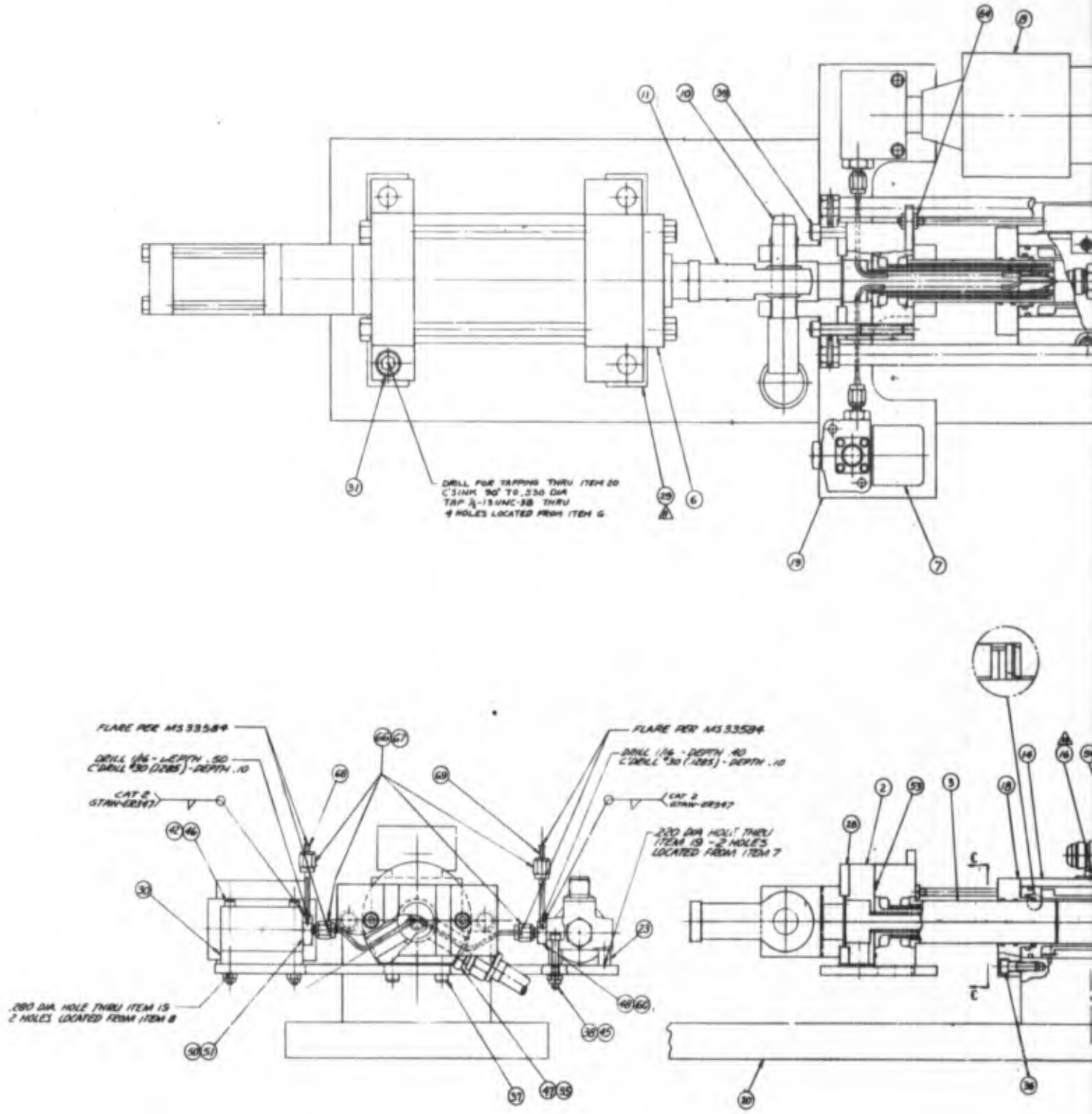

Figure

Photo-Reduced Drawing of Mov
Thiokol-RMD Drawi

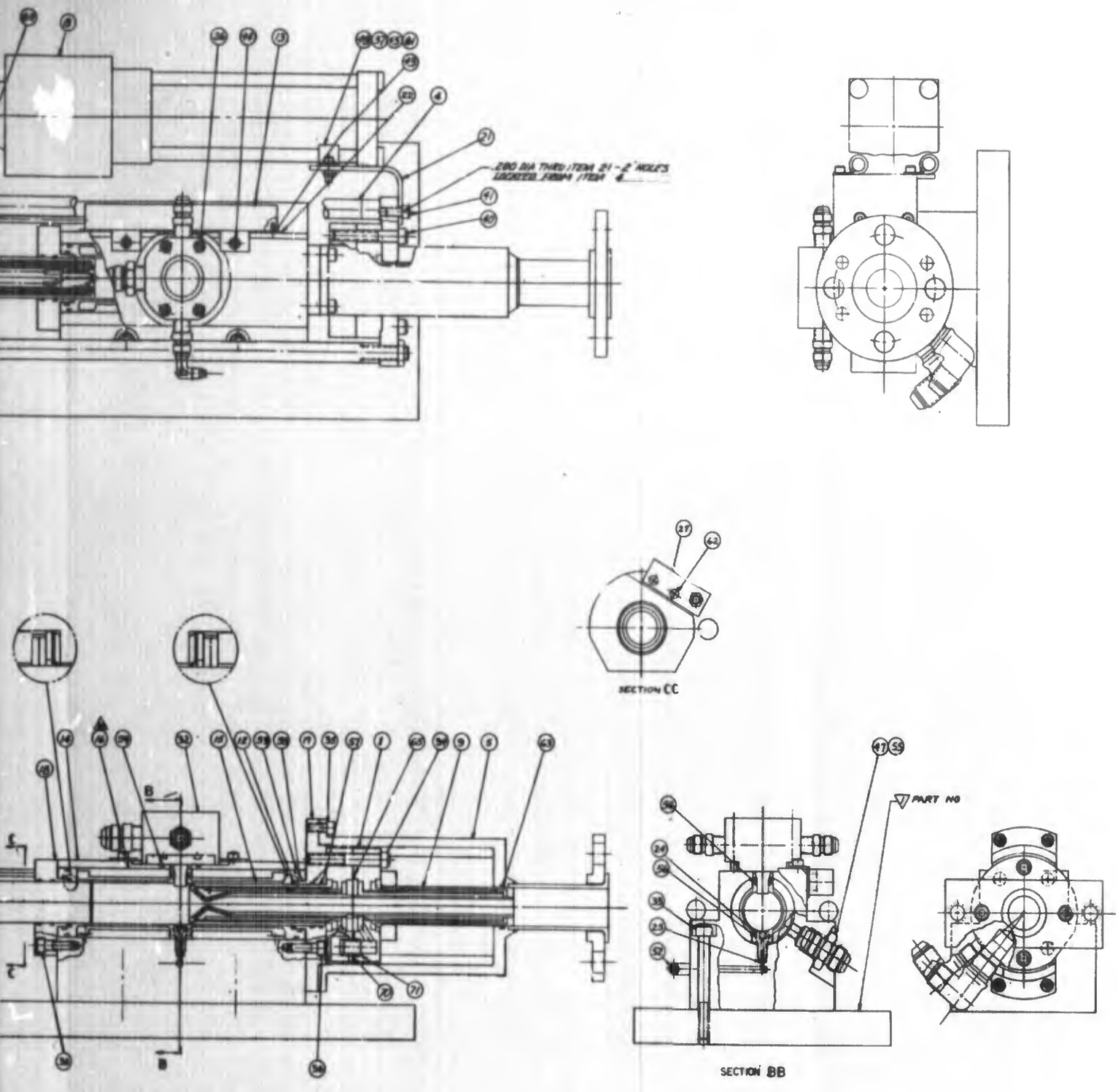

Figure 1

ing of Movable Combustion Chamber
RMD Drawing X315513

4. PHASE II - DEMONSTRATION TEST PROGRAM

The purpose of a demonstration test program for the movable combustion chamber was to verify that all critical aspects of the system operated satisfactorily. Actuation during firing, suitable sealing at all times, adequate cooling of all components and reasonable combustion performance were to be demonstrated. This effort, as well as the fabrication of the system, comprised Phase II of the program.

4.1 Laboratory Test Setup

Demonstration tests were conducted with chlorine pentafluoride and hydrazine. The laboratory test setup consisted of pressurized tank supplies of each propellant and the conventional regulatory and flow control equipment for these propellants. An additional fluorine passivation system was needed to prepare the chlorine pentafluoride lines. An overall view of the movable combustion chamber test setup is shown in Figure 3. The engine was fired into a 1000 ft^3 vacuum tank through a 12 inch flange which was the cover of a port in the side of the vacuum tank.

The oxidizer feed system contained the 180° loop of 1/4 inch copper line seen in the left of the picture. A rigidly mounted safety valve was at one end of the loop while the main propellant valve which moved with the traversing frame of the chamber was at the other end of the loop. The semi-circular loop of the larger flexible hose, which was also required to move with the engine, was one of the coolant water passages. Aside from the flexible lines required for chamber movement, most aspects of the test stand were conventional for these propellants.

A more detailed view of the engine mounted in position for firing is shown in Figure 4. The propellant valves can be seen on the movable frame. The large valve mounted parallel to the axis of the engine is the main oxidizer valve. This type of valve, manufactured by Control Components, Inc. was chosen for its unique seal design which is especially well suited for use with interhalogens. The actuating cylinder for the oxidizer valve required a separate pneumatic 4-way actuating valve which can be seen in the lower right of Figure 4. This valve was rigidly mounted and not carried by the moving engine frame. The small Marotta MV100WD main fuel valve is in the upper right of Figure 4.

Figure 3
Movable Combustion Chamber Test Setup

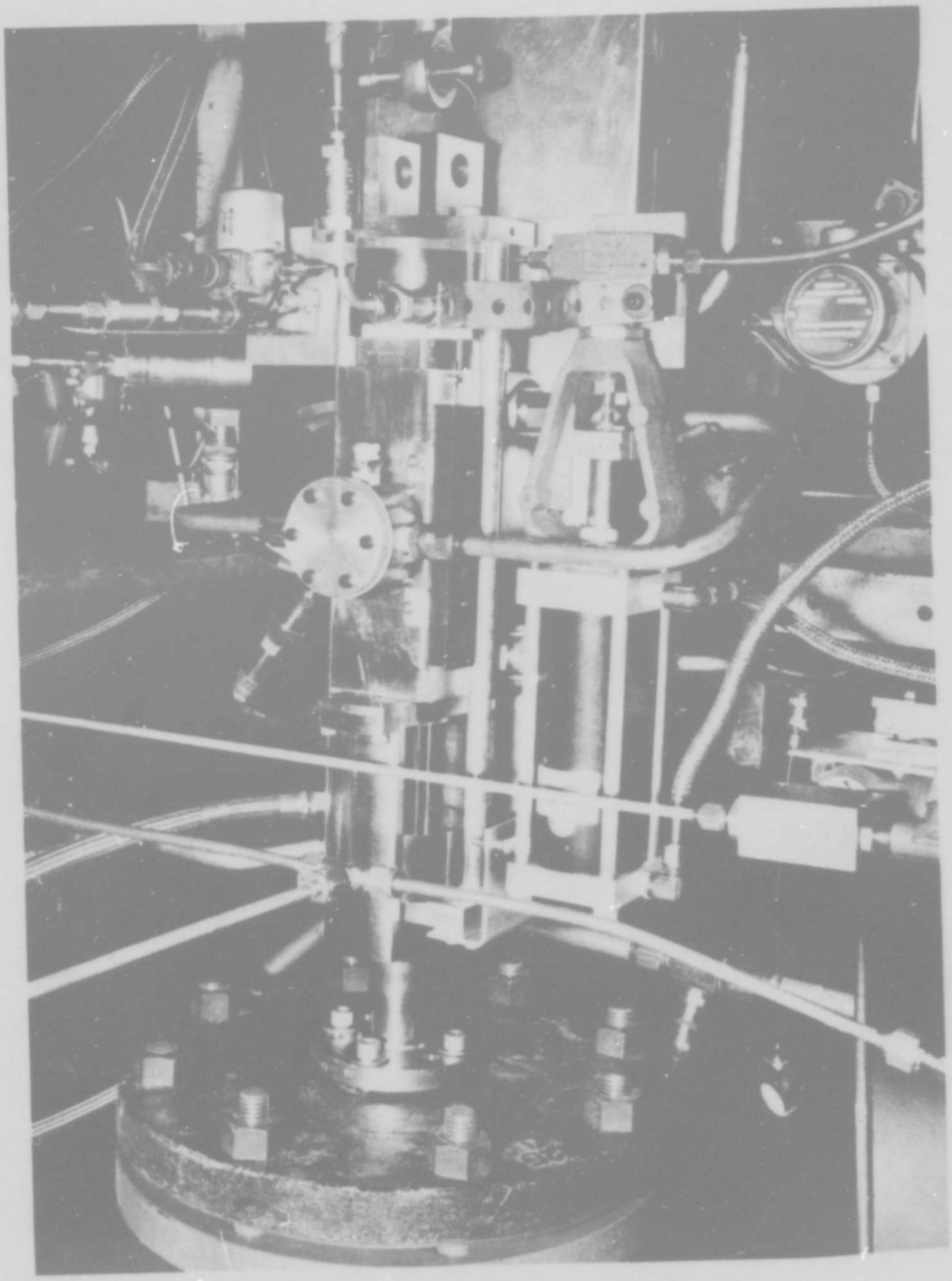

Figure 4
Close-Up Photograph of Movable Combustion Chamber
In Position For Firing

In all tests, a government furnished mass-spectrometer bleeder (or probe head) was mounted on the engine and sealed off so that there was no continuous flow of combustion gases into the laboratory. Chamber coolant water was also used to cool this component. In Figure 4, the 1/2 inch lines leading into and out of the masspec bleeder can be clearly seen.

Instrumentation consisted of a chamber pressure transducer, two injector inlet pressure transducers, dial gauges in the pressurizing systems to measure propellant tank pressures, six thermocouples measuring inlet and outlet temperatures in three coolant water channels, and a position indicating potentiometer to give the instantaneous position of the chamber. Main propellant valve currents were also monitored to determine the durations of starting and stopping transients. Coolant water flowrates in each of the three coolant circuits were measured by turbine type flow meters.

A single 60 gallon pressurized water tank was used to supply all three coolant water circuits. In all tests, the flowrates were maintained as follows:

Injector cooling jacket	1.32 - 1.35 lb/sec
Chamber cooling jacket	0.52 - 0.53 lb/sec
Nozzle throat and extension tube	2.03 - 2.07 lb/sec.

The transient time for filling injector volumes was calculated to permit biasing the electrical signals to the main propellant valves. It took approximately 0.25 seconds longer to fill the oxidizer injector volume; therefore, the oxidizer valve was energized 0.25 seconds prior to the fuel valve in all tests.

4.2 Test Results

All tests made with the movable combustion chamber are summarized in Table III. The test program gradually increased the severity of the environment within the chamber, culminating in a 60 second test at chamber pressure equal to 455 psia and O/F equal to 3.2.

Table III

Summary of Demonstration Test Results

Test No.	Chamber Pressure (psia)	Half Amplitude P_{ch} Var. (psi)/%	Run Duration (sec)	Mixture Ratio (O/F)	c* (ft/sec)	ΔT Ch. (°F)	ΔT Noz (°F)
A-2	30	--	2.0	3.3	-	7	0
A-3	253	11 / 4.4	2.1	3.7	5430	6	5
A-4	236	15 / 6.3	4.8	3.8	4940	18	9
A-5	355	17 / 4.8	10.0	3.4	6175	18	12
A-6	432	25 / 5.8	10.7	3.2	5130/5230	8	20
A-7	455	22 / 4.8	60.0	3.2	5560/6040	11	19

Initial tests were made at flowrates much lower than the design flowrates. Poor injector characteristics under these conditions resulted in very erratic performance in Test A-2. As the flowrates were increased in subsequent tests, engine operation improved.

Chamber pressure variations were monitored as a part of the routine data reduction. Chamber pressure fluctuated at relatively low frequencies at amplitudes of approximately ± 5 percent of the mean level. No high frequency response instrumentation was employed.

During runs A-4 and A-6, the injector and exhaust nozzle were moved together from one extreme of the chamber to the other. No leakage of any kind was noted in these tests or any other tests.

The two values for c* shown for Tests A-6 and A-7 were measured at the beginnings and just prior to the ends of the tests.

The temperature transient for all components of the movable combustion chamber covered a period of about two seconds. After that time, the coolant water ΔT was constant and thermal steady-state prevailed. The nozzle coolant water ΔT varied almost

directly with chamber pressure as shown in Table III. Chamber coolant temperature increases were not as consistent, possibly because of injector spray patterns which were not always concentric. Propellant impinging and reacting on the chamber wall in Tests A-4 and A-5 may have caused higher than normal heat transfer rates. In all tests, the temperature rise of the injector coolant water was negligible.

In Test A-6, a failure of the exhaust tube mounting bracket was experienced due to two conditions. An external cooling water spray was not properly directed and did not cool the tube sufficiently. In addition, the pressure at the outlet of the tube was extremely low, forcing the exhaust gases to expand and impinge directly upon the inside of the tube. After shutdown, the two conditions were corrected and the burned-through tube was repaired with masking tape for the next test. The very low vacuum tank pressure was unique to the operation of our facility and would not be attained in RPL tests.

The 60 second test, A-7, was made at the most severe environment that the movable combustion chamber is required to withstand. At the experimental mixture ratio and chamber pressure, the adiabatic flame temperature of ClF_5/N_2H_4 is in excess of 4000°K (6700°F)

At the conclusion of Test A-7, the exhaust nozzle was slightly eroded with a throat area increase of about 13 percent over the course of the testing program. An enlarged sketch of the throat obtained from an optical comparator is shown in Figure 5. Non-uniformity of the enlargement was probably due to distorted injector spray characteristics. Slight and continual enlargement of the throat is to be expected with ClF_5/N_2H_4 at the extreme conditions of these tests.

Injector water flow calibrations were made before, during and after the testing program. Figure 6 shows how both the fuel and oxidizer channels enlarged. The physical separation of injector and cooling jacket may have resulted in undue heating of the nickel injector leading to the erosion.

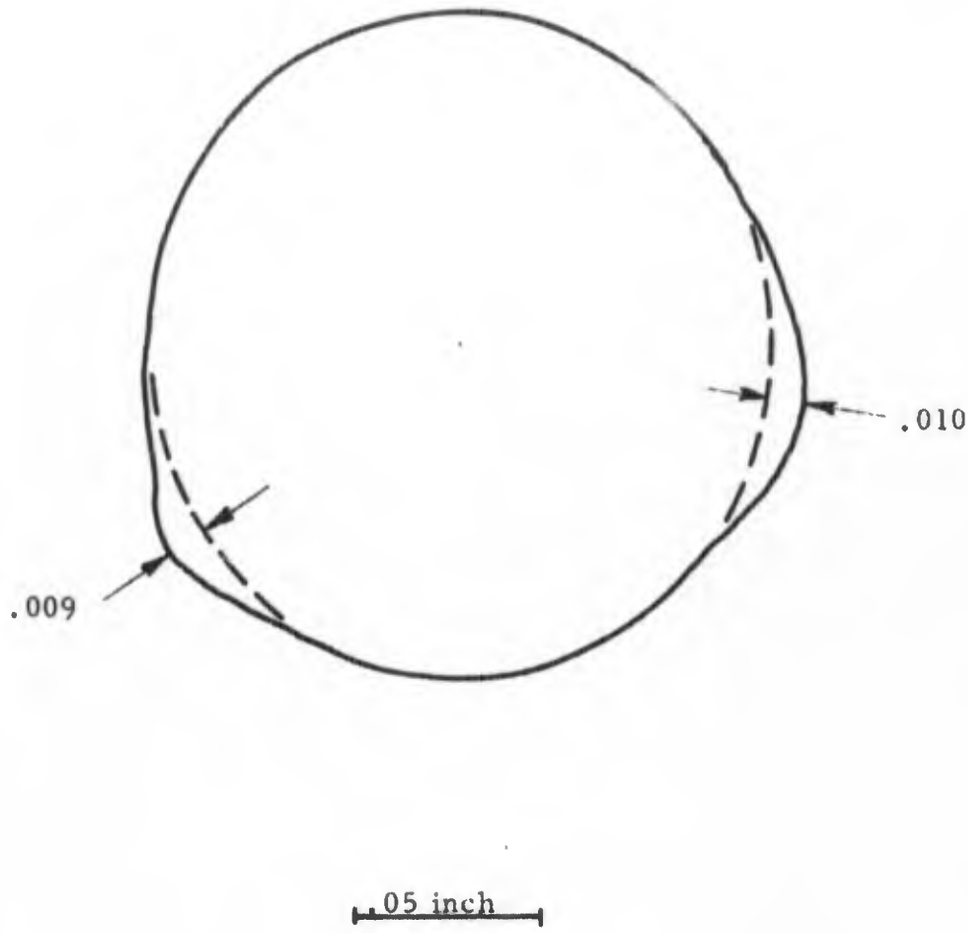

Figure 5
Post-Test Nozzle Throat Cross-Section

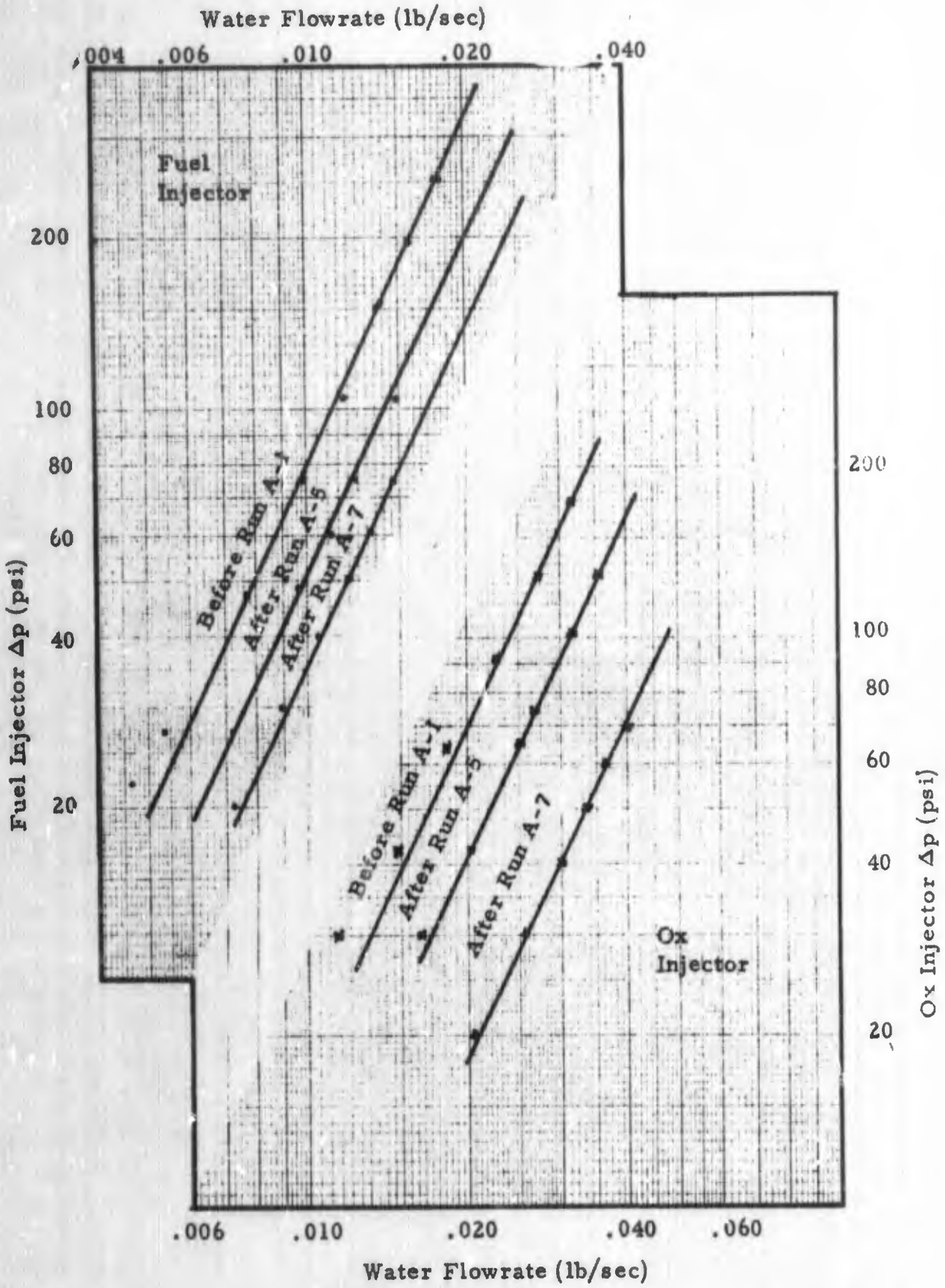

Figure 6
Injector Water Flow Calibrations

5. PHASE III - CHARACTERISTICS OF THE RPL/ROCKETDYNE PROBE

5.1 Introduction to the Present Probe Analysis

In studies of propellant combustion recently reported from Edwards Air Force Base, Rocket Propulsion Laboratory (5, 6, 7), a gas sampling probe system was employed which was designed as part of a complete laboratory facility (8). The movable combustion chamber described in the previous sections was designed to be mated to this gas sampling system. Briefly, the gas extraction system takes gases at combustion chamber conditions (up to 500 psia) and transports them through differentially pumped orifices or skimmers to a mass spectrometer operating at about 1×10^{-6} torr, an overall pressure ratio of more than 10^{10}. It should be noted that sampling from this high pressure presents a variety of problems. The very high temperatures are a source of additional problems and complication.

Figure 7, taken from (8), shows the general arrangement of the major components required for gas sampling. The gases travel from the combustion chamber (probe tip) to the ionization region of the mass spectrometer in a direct line of sight forming a molecular beam.

The probe tip extends through the cooled wall of the combustion chamber and is an integral part of the main probe assembly as sketched in Figure 8. Gases enter the probe through a rectangular slot, .003 x .030 x .375 inch long. Two skimmers (.003 inch and .010 inch diameter orifices) serve to separate chambers of successively lower pressure. Pressures at each location as reported by Rocketdyne (8) are shown in the figure. The molecules traveling through the probe are collimated by the skimmers and the beam is ionized by electron bombardment in the ionization region of the mass spectrometer. Pulsed electrical and magnetic fields in the mass spectrometer then accelerate the ions for their flight down the drift tube to be electrically detected and recorded.

The problem inherent with all sampling, which must be overcome in any probe design, is that the sample should not be altered during flow through the probe, specie concentrations should not change either by selective removal or by generation of spurious species, and that the source should not be affected by extracting a sample.

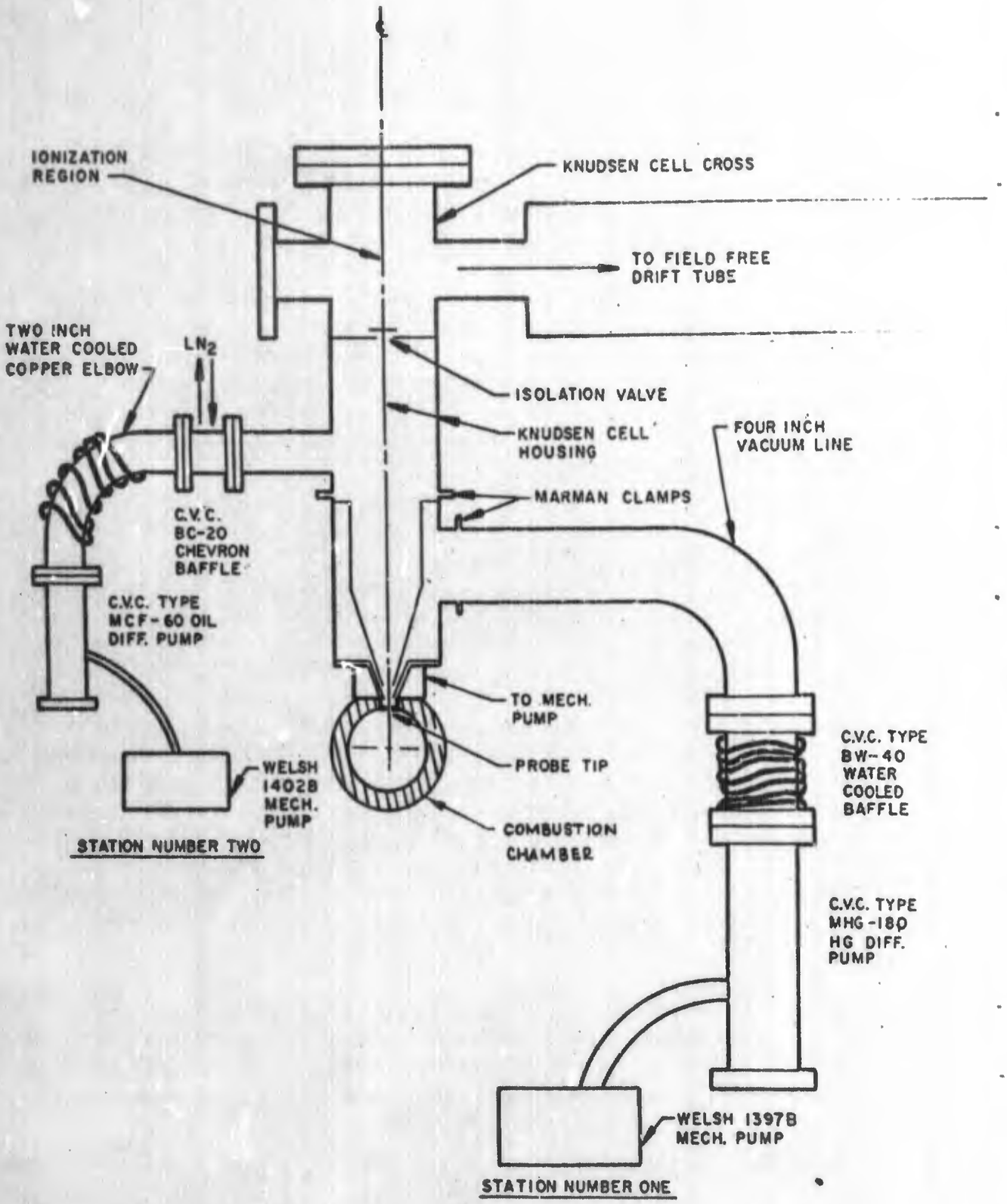

Figure 7
Block Diagram of Gas Sampling System Pumping Stations (Ref. 8)

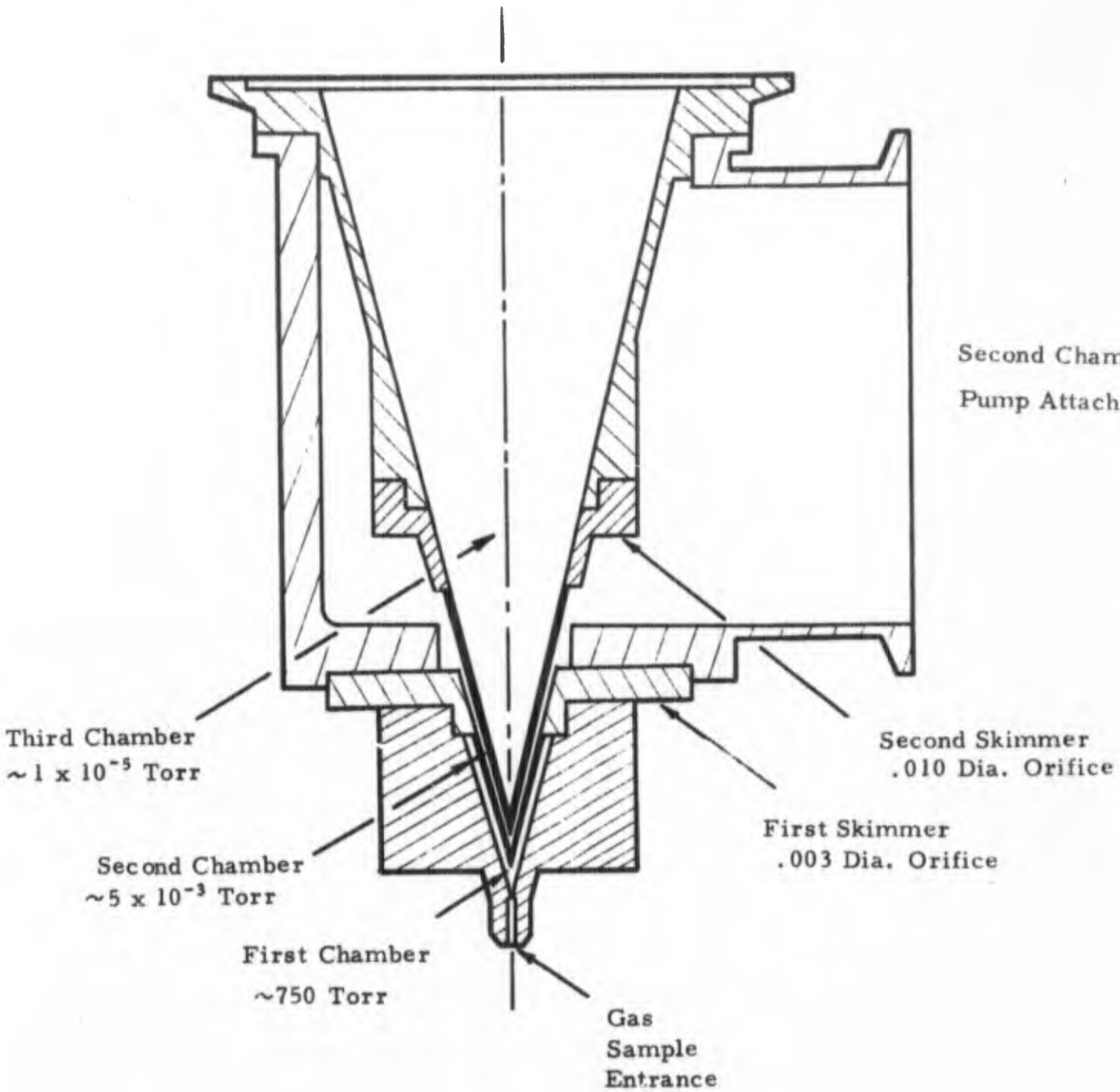

Figure 8

Assembly of Gas Sampling Probe (Ref. 8)

The discussions that follow examine at each stage of the probe the local condition of the sampled gases. Initially, the sample flows into the probe through a constant area cooling channel. Entrance conditions affecting flow into the present probe are briefly discussed in 5.2.1. A generalized discussion of compressible flow with combined heat transfer and friction is given in 5.2.2. Since the boundary conditions for the channel flow problem were not known, iterative calculations were used to define the overall probe and cooling channel behavior. The calculations employed a three-dimensional conductive heat transfer program for the channel walls and a compressible flow program for the channel flow. The three-dimensional heat transfer procedure is described in 5.2.3. Finally, in 5.2.4, the compressible flow program is described and the behavior of constant composition gases flowing through the cooling channel of the present RPL/Rocketdyne probe is predicted for ClF_5/N_2H_4 and for N_2O_4/N_2H_4.

With the non-reactive gas calculations available, it is possible to estimate whether the combustion chamber species will remain in equilibrium as local conditions change or will freeze due to the rapid temperature and pressure drops. These questions are considered in 5.3.

Upon emerging from the cooling channel, the gases expand in an unconfined free-jet whose characteristics are described in Section 5.4.

After summarizing other probe/gas phenomena in 5.5 and 5.6, areas of possible improvement for future gas sampling endeavors are discussed in Section 6.

5.2 Dynamics of Channel Flow

5.2.1 Gas Flow at the Channel Entrance

The inlet to the gas extraction probe is located within the wall of the combustion chamber, protruding slightly but otherwise resembling a static pressure tap. Since the flow into the probe (as calculated later) is a very small fraction of the total flow through the chamber, no disturbance of chamber dynamics will occur.

It is possible that a small bias in the sample could occur because the gases are taken from the chamber wall and may be slightly different from the gases in the center of the combustion chamber. The rectangular flow channel in the probe, however, has a 10/1 aspect ratio with the long dimension aligned parallel to the combustion chamber centerline. Presumably,

gases entering the probe channel may consist of some chamber boundary layer species on the upstream side of the channel but the main part of the flow will be taken from the turbulent center core. If stream tubes are maintained throughout the length of the channel, the outer portions of the channel flow will be "skimmed off" in any event. Since Reynolds number just after the entrance to the probe channel is only slightly over 2000, it is likely that there will not be a great deal of turbulence and mixing within the channel. Due to the decrease of gas pressure and temperature in flowing through the channel, viscosity decreases, density increases slightly and although Mach number increases, velocity decreases. The effect of these changes is that Reynolds number at the outlet increases to over 3000 indicating again that a great deal of turbulence will not be encountered.

Sample bias due to combustion chamber boundary layer effects is therefore not likely.

5.2.2 Generalized Channel Flow Dynamics

Details of the present RPL/Rocketdyne gas sampling probe are given in (8) and on Edwards Air Force Base Drawing X66F18257 "Mass Spectrometer Bleeder". An enlarged sketch of the inlet is shown in Figure 9. The effective flow channel is a highly-cooled slit milled into a split copper rod. Since it is impossible to estimate a priori for a channel in which large heat losses occur and in which viscous friction is present which of the competing effects will predominate, a careful analysis of two and three dimensional conductive heat transfer was combined with the channel gas flow dynamics to determine channel outlet conditions.

In a constant-area, adiabatic duct with subsonic flow, friction has the net effect of accelerating the gases, decreasing their density, temperature and stagnation pressure. For this so-called Fanno flow, there is no heat transferred from the gases and the stagnation temperature remains constant. On the other hand, in a gas flowing through a constant-area duct without frictional effects but involving heat transfer and thus the stagnation temperature , a new formulation of the problem results in a locus of states known as a Rayleigh flow. For example, with subsonic flow in a channel which is extracting heat from the gases, stagnation temperature decreases, as does velocity. Stream pressure and stagnation pressure both increase in a cooling process , however, this effect requires frictionless flow. The value of stream temperature goes through a maximum which is a function of Mach number causing an apparently anomolous situation, viz. for air at values of M between .85 and 1, heat rejection acts to <u>increase</u> stream temperature. (9)

These processes are summarized in Table IV.

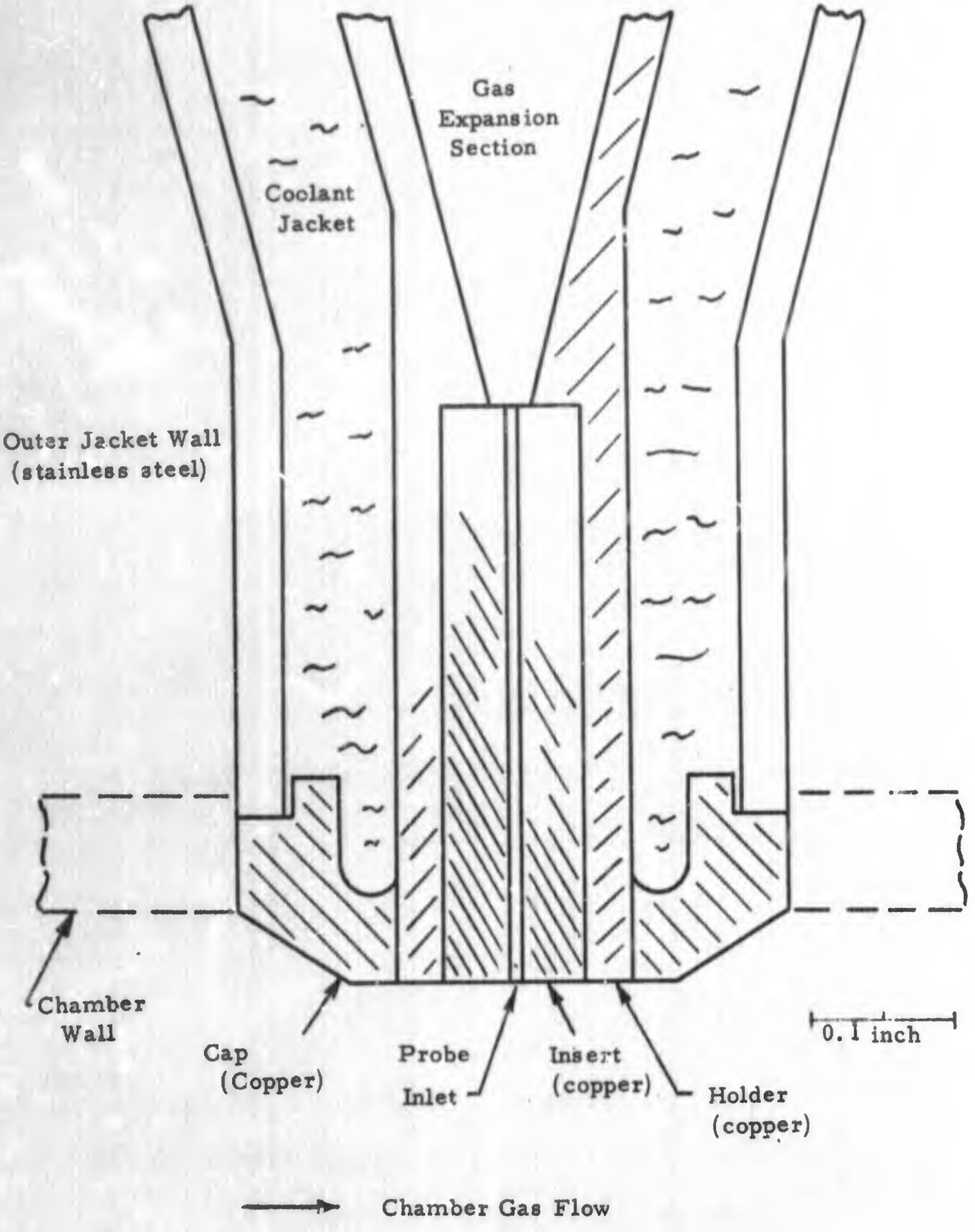

Figure 9

Sketch of Present RPL/Rocketdyne Gas Sampling Inlet

Table IV

Summary of Gas Parameters in Subsonic Flow Through a Constant-Area Duct

	Adiabatic Flow With Friction	Cooling With No Friction
Velocity	increases	decreases
Mach Number	increases	decreases
Stream Pressure	decreases	increases
Stagnation Pressure	decreases	increases
Stream Temperature	decreases	decreases for $M<1/\sqrt{\gamma}$ increases for $M>1/\sqrt{\gamma}$
Stagnation Temperature	constant	decreases

Thus, the simultaneous processes involved in frictional flow and heat rejection compete with each other and the dominating process will determine the state of the gases at the outlet of the channel.

In a rigorous analysis of the probe inlet channel, the problem is compounded by the convective and radiative heat transfer from the combustion chamber gases and walls to the exposed probe tip, as well as by the problem of cooling the sampled gases passing through the water jacketed probe. In order to determine the extent which boundary conditions affect gas flow dynamics, the overall probe heat transfer problem will be examined first and the channel gas dynamics subsequently.

5.2.3 Three Dimensional Heat Transfer Analysis of Probe Tip

Heating of the end of the probe tip is essentially independent of the gas flow. This influence can readily be determined and expressed in terms of convection and radiation boundary conditions. As shown in Figure 9, the probe tip consists of:

- a probe-end which is exposed to the chamber gases and receives a combined convective and radiative heat input,
- a convectively heated copper insert with extreme gas temperature variation with length,
- a highly turbulent convective coolant water flow over the holder and cap.

These boundary conditions were evaluated in a transient three dimensional heat transfer digital computer program (RMD No. D0039) which uses the following form of the conduction equation with convection and radiation heat inputs:

$$T_n' = T_n + \frac{\Delta \tau}{\rho c V} \left[\sum_i \frac{(kA)_i}{\Delta x_i} (T_i - T_n') + Q_c + Q_r \right]$$

In the use of this equation, the temperature at a node is determined by the simultaneous effects of conductive, convective and radiative inputs.

The analyses used information from the following sources;

Theoretical combustion gas products and gas temperature	RMD Thermochemical Computer Program D0001
Gas transport properties	NASA TR R-81 (10) NASA TR R-132 (11)
Probe Wall thermal properties	Eckert and Drake (12)

Values of most of the parameters used in the analyses are shown in Table V.

For the purpose of the heat transfer analysis, the probe was represented by a conduction network consisting of nine interconnected nodes and by six additional nodes to represent the combustion gas, the channel sample gas and the cooling water. The nodal arrangement is shown in Figure 10.

The values used for thermal properties for the copper and steel components of the probe are as follows:

Material	Thermal Conductivity (Btu/ft hr F)	Density (lb/ft^3)	Specific Heat (Btu/lb-F)
Copper	200	558	0.09
Stainless Steel	10	500	0.11

Table V

Gas Concentrations and Properties Used in Channel Analysis

Combustion Gases

ClF_5/N_2H_4 Gas	Mole Fraction	N_2O_4/N_2H_4 Gas	Mole Fraction
Cl	.06833	H	.01110
ClH	.05492	HO	.03643
F	.03009	H_2	.05605
HF	.58765	H_2O	.46436
H	.04805	NO	.01133
H_2	.02533	N_2	.40250
N_2	.18522	O	.00421
		O_2	.01399

	ClF_5/N_2H_4	N_2O_4/N_2H_4
Maximum Temperature (F)	6848	5284
Molecular Weight	22.059	21.242
Ratio of Specific Heat	1.18	1.22
Specific Heat (Btu/lb F)		
@ 2000 F	0.33	0.56
@ 4000 F	0.36	0.62
@ 6000 F	0.38	0.64
Viscosity (lb/in-sec) x 10^5		
@ 2000 F	0.27	0.27
@ 4000 F	0.41	0.42
@ 6000 F	0.52	0.54
Chamber Heat Transfer Coefficient (Btu/hr ft^2F)		
Convection	46.1	46.1
Radiation	0*	28.6

* Gases are transparent, hence no radiation

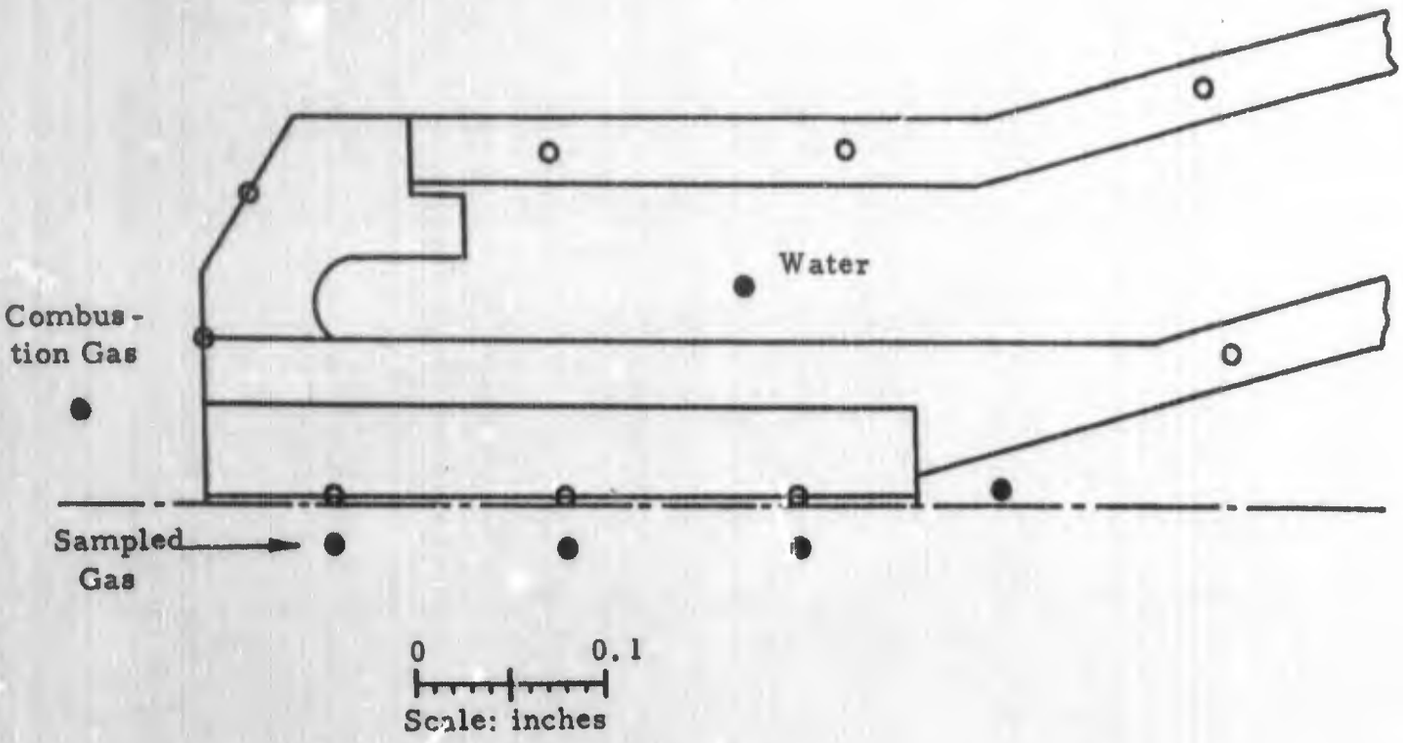

○ Nodes linked by conduction

● Nodes representing gas and coolant boundary conditions

Figure 10

Three-Dimensional Heat Transfer Nodal Network

The 3-D program was used in conjunction with the gas dynamics program described in the next section. With an initial arbitrarily selected decay of gas-temperature and pressure in the flow through the cooling channel, the 3-D program provided the temperature variation along the channel walls. With these wall temperatures, the gas dynamic equations were employed to determine an improved estimate of gas properties in the channel.

The new gas properties were then recycled through the 3-D program and the procedure repeated several times. If desired, this iteration could have been performed automatically by computer by writing the necessary transition program, however, for the present application it was performed manually.

Probe temperature distributions for two propellant systems, ClF_5/N_2H_4 and N_2O_4/N_2H_4, are shown in Figures 11 and 12.

Comparing Figures 11 and 12, we see that the propellant system which radiates (N_2O_4/N_2H_4) results in higher probe surface temperatures, even though the combustion gas temperature is lower than for ClF_5/N_2H_4. Wall temperatures in the cooling channel are seen to vary by about 200°F for both propellant systems. It will be seen later that wall temperature variations of this magnitude have little effect on outlet gas properties. Therefore, the precision to which the cooling channel wall temperature is known is relatively unimportant.

5.2.4 Compressible Flow Through a Constant Area Duct

The cooling channel of the gas sampling probe is a rectangular duct .003 x .030 inches. Use of the effective diameter (4 x flow area/wetted perimeter) gives an L/D of almost 69, a relatively long channel. The pressure drop through this passage results from the simultaneous action of friction and heat transfer. Rough calculations quickly show that the flow is choked, the Mach number at the exit of the channel is therefore unity, and that the flow at all other points in the channel is subsonic.

In order to analyze this problem, we assume for our constant area duct that the specific heat and molecular weight are constant and that the flow is one-dimensional, i.e., all properties are constant at any cross-section.

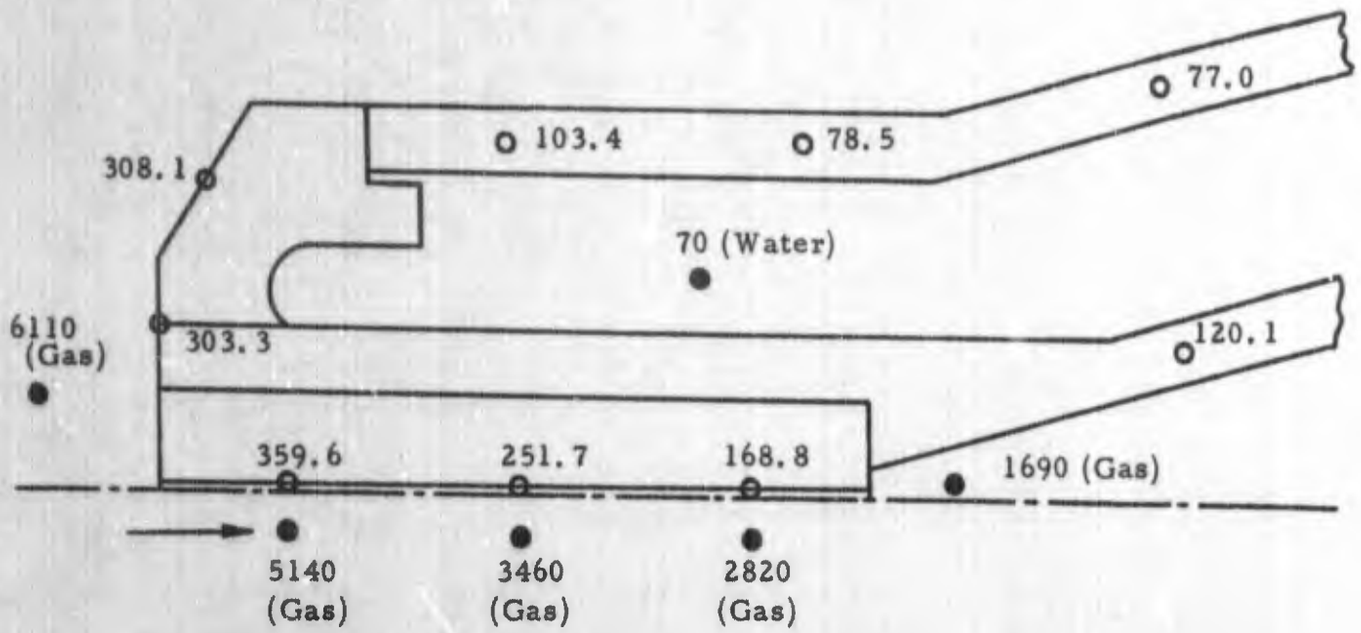

Note: Temperatures (^{o}F)

Figure 11

Probe Temperature Distributions
ClF_5/N_2H_4 at O/F = 2.70 and P_c = 500 psia

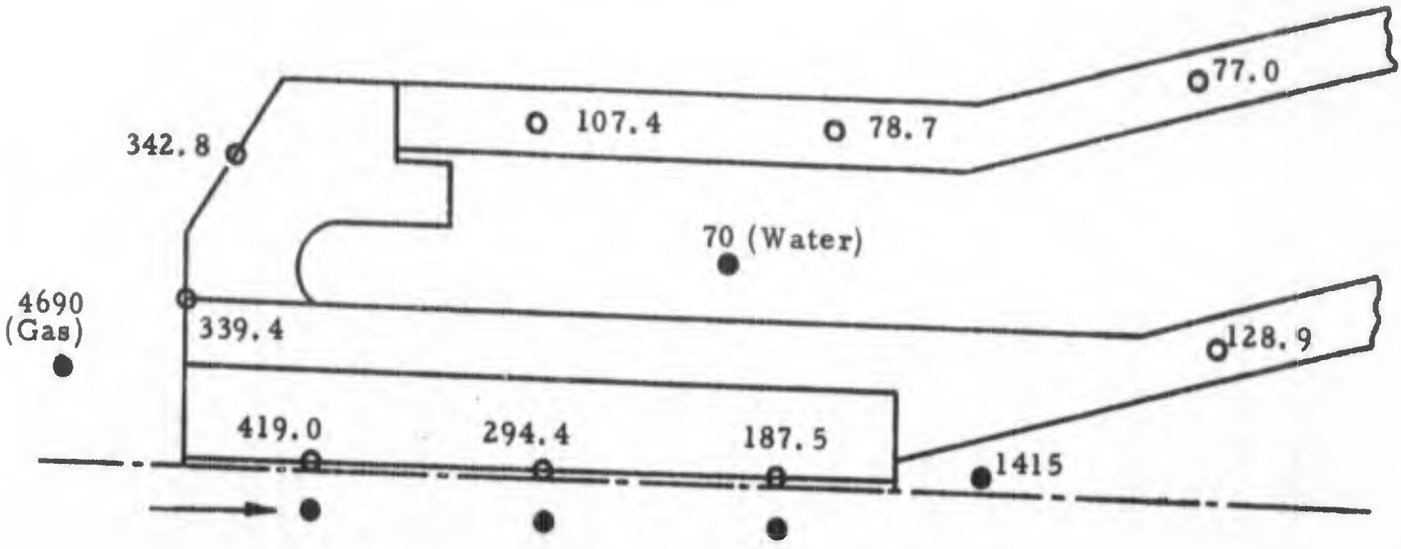

Note: Temperatures (^{o}F)

Figure 12

Probe Temperature Distributions
N_2O_4/N_2H_4 at O/F =1.44 and P_c=500 psia

For these restraints, the generalized flow equation (9) reduces to

$$\frac{dM^2}{M^2} = \frac{(1+\gamma M^2)(1+\frac{\gamma-1}{2}M^2)}{1-M^2}\frac{dT_o}{T_o} + \frac{\gamma M^2(1+\frac{\gamma-1}{2}M^2)}{1-M^2}\frac{4f}{D_h}dx$$

For simplicity, the coefficients for temperature change and frictional loss are put in influence coefficient form with F_{T_o} for the temperature and F_f for friction. Then,

$$dM^2 = F_{T_o}\frac{dT_o}{T_o} + F_f \; 4f \; \frac{dx}{D_h}$$

This equation can only be formally integrated in special cases through a relation linking the friction and heat transfer terms. Following Shapiro (9), we take the adiabatic wall temperature to be the same as the stagnation temperature, implying a recovery factor of unity. In addition, Reynolds Analogy between friction and heat transfer is employed in the form

$$\frac{h}{c_p V \rho} = \frac{f}{2}$$

There is sufficient experimental and theoretical justification for applying these relations in many cases. In particular, Reynolds Analogy is applicable for;

a. highly turbulent flow, any Prandtl number,
b. low Reynolds number flow, Prandtl number unity, or
c. Prandtl number unity, equal eddy diffusivities for heat and momentum (13).

Although our flow conditions meet only marginally any of the above criteria, simplicity and ease of computation recommend use of this analogy even though a slight uncertainty in accuracy may result.

By considering the change in gas temperature to be related to the convective heat transfer in the duct of infinitesimal length, dx, the change in temperature may be expressed as

$$\frac{dT_o}{T_w - T_o} = \frac{1}{2}\frac{4f\,dx}{D_h}$$

If the friction factor, f, is known locally, the change of total temperature may be calculated as

$$\frac{T_{o_2}}{T_{o_1}} = \frac{T_w}{T_{o_1}} - \left(\frac{T_w}{T_{o_1}} - 1\right) \exp\left[-\frac{1}{2}\frac{4f\Delta x}{D_h}\right]$$

In order to calculate the friction factor, the local Mach number must be known, to determine Reynolds number. Substituting in the above,

$$dM^2 = \frac{F T_o}{T_o} + \frac{2F_f}{T_w - T_o} dT_o$$

an equation which is solved numerically by evaluating the change in Mach number between stations 1 and 2 separated by a defined, small distance. The solution in terms of influence coefficients evaluated at the average Mach number for the section is:

$$M_2 = \sqrt{M_1^2 + \Delta M^2}$$

$$\text{where} \quad \Delta M^2 = 2\left(\frac{T_{o_2}}{T_{o_1}} - 1\right)\left[\frac{\bar{F} T_o}{\frac{T_{o_2}}{T_{o_1}} + 1} + \frac{2\bar{F}_f}{2\frac{T_w}{T_{o_1}} - \frac{T_{o_2}}{T_{o_1}} - 1}\right]$$

The solution for this numerical form was programmed for a digital computer because a great number of calculations were required to consider small section lengths and to make the iterations necessary to arrive at simultaneous agreement of average section Mach number with the friction factor and influence coefficients. The program was constructed to predict outlet Mach number, temperature and pressure for a given inlet Mach number, temperature, pressure, properties, probe channel dimensions and estimated wall temperature. Because of this simple structure a range of Mach number inlet conditions were required to find the inlet Mach number which would satisfy the choked flow outlet condition. From the program output (i.e., mass flux, Reynolds number, etc.) heat transfer coefficients were computed for use in the three dimensional heat transfer analysis described previously in order to refine the estimation of probe channel wall temperature.

The results of the calculation for two propellant systems are as follows:

Propellants	ClF_5/N_2H_4	N_2O_4/N_2H_4
O/F	2.70	1.44
Combustion chamber gas temperature (assumed c* = 95 %) (°F)	6117	4690
Combustion chamber pressure (psia)	500	500
Exit total temperature (°F)	2090	1622
Exit static temperature (°F)	1649	1415
Exit total pressure (psia)	287	302
Exit static pressure (psia)	166	169
Residence time in probe (sec)	14×10^{-6}	14×10^{-6}

Gas temperature and pressure variations for the calculated flow of ClF_5/N_2H_4 combustion products are shown in Figures 13 and 14.

Figures 15 and 16 correspond to the above but for N_2O_4/N_2H_4 propellants.

In these calculations, the energy released during possible recombination of free atoms has been neglected. The flow of gases has been assumed to remain at constant composition.

The iteration between the three dimensional heat transfer program and the gas dynamic calculation as described in 5.2.3 showed that a step-wise wall temperature distribution had little effect on outlet gas properties This additional complexity was therefore neglected in most computations. Additional results with slightly altered geometry or different coolant temperature with the same basic cooling channel design are described in Section 6.1.

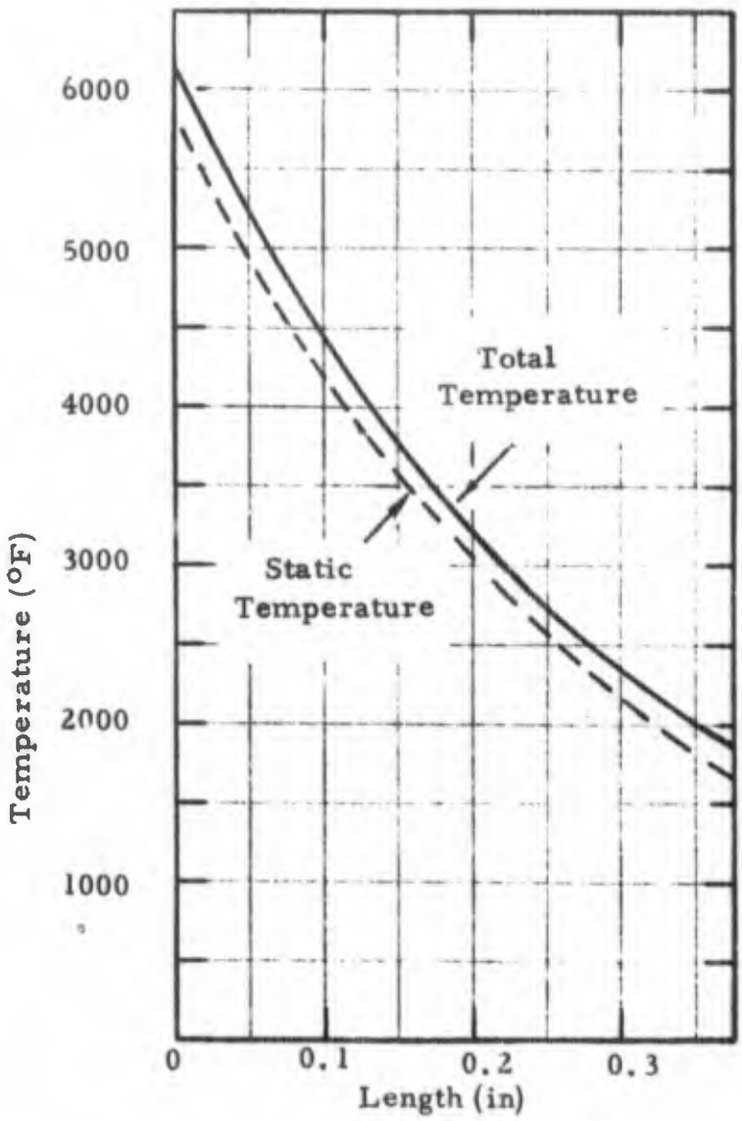

Figure 13

Gas Temperature Variation With Channel Length
ClF_5/N_2H_4 at O/F=2.70 and Pc=500 psia

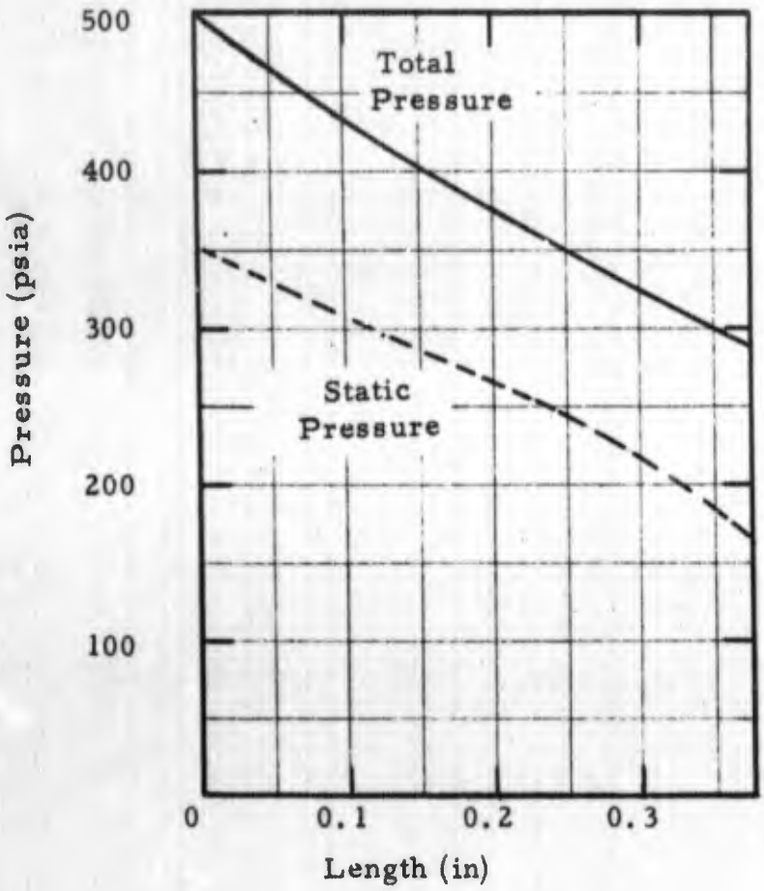

Figure 14

Gas Pressure Variation With Channel Length
ClF_5/N_2H_4 at $O/F = 2.70$ and $P_C = 500$ psia

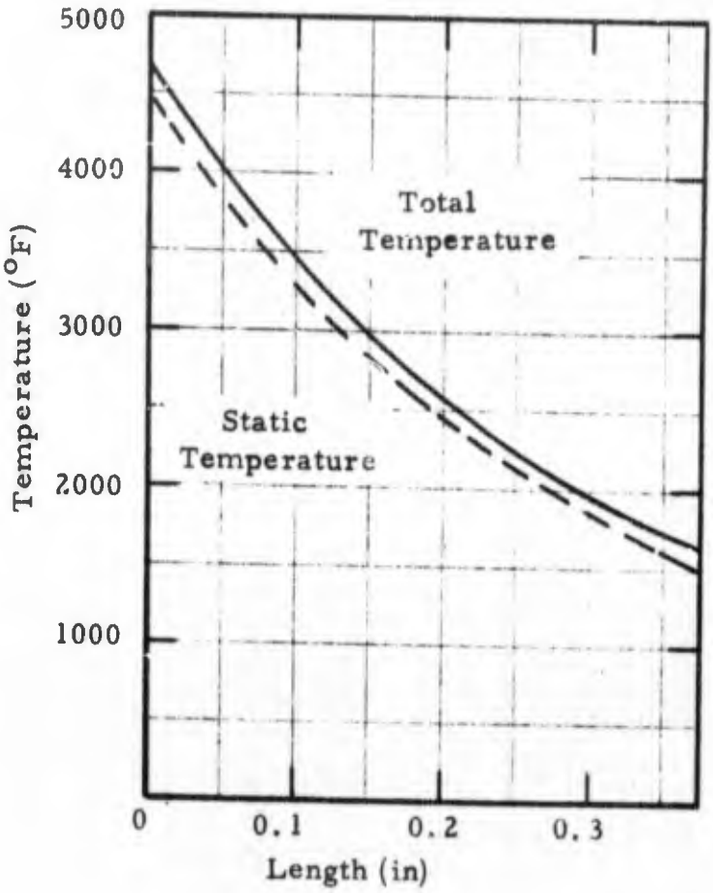

Figure 15

Gas Temperature Variation With Channel Length
N_2O_4/N_2H_4 at O/F = 1.44 and P_c = 500 psia

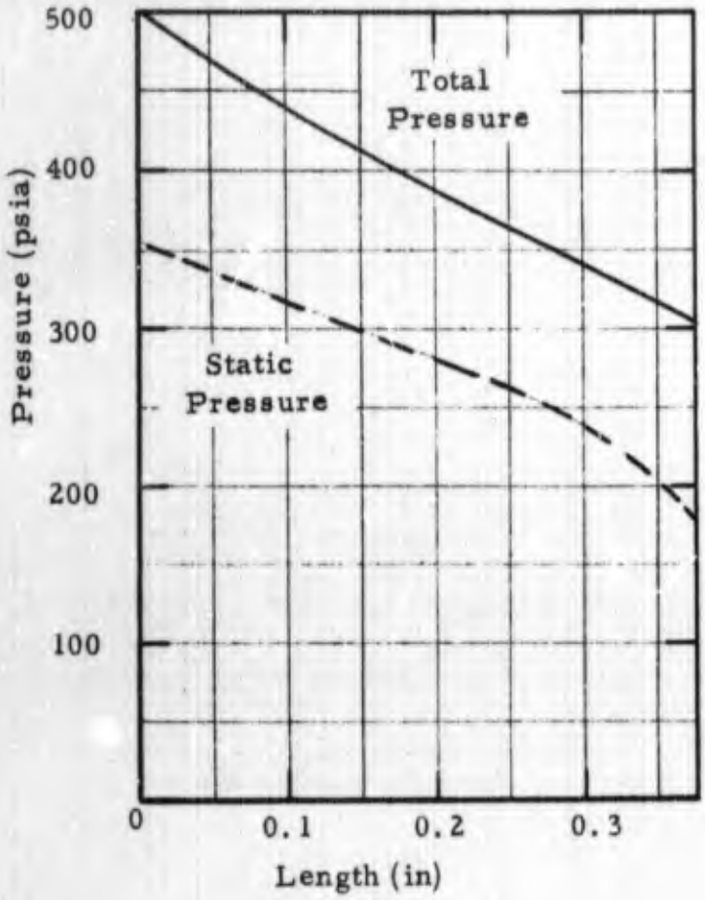

Figure 16

Gas Pressure Variation With Channel Length
N_2O_4/N_2H_4 at O/F =1.44 and P_c=500 psia

5.3 Chemical Kinetics of Channel Flow

The ideal gas sampling probe extracts a small quantity of gases from a reaction zone without disturbing it, quenches and freezes chemical reactions before significant changes occur, and preserves specie concentrations for subsequent analysis. Historically, this has been done in the case of sampling from low pressure flames by rapid expansion into collision-free flow. When this approach is attempted from high pressure sources, pumping requirements may be excessive and/or impractically small orifices may be required. As pointed out by Rocketdyne (8), the mean free path of an air molecule at 500 psi and 4000°F is 1.85×10^{-6}cm. Transporting these molecules without chemical change to a region where the mean free path is of the same order as characteristic geometric dimensions is a difficult problem. Sampling from a high pressure source therefore requires approaches more sophisticated than simple free jet expansion; the Rocketdyne/RPL probe is one possible approach.

5.3.1 High Pressure Sampling Problems

A gas sampling probe extracting a reacting mixture from a high temperature, high pressure region presents a formidable problem in minimizing composition changes. Exact calculations of multicomponent reacting flow fields require machine solutions to be practical; however, a number of approaches are possible to approximate probe gas handling characteristics. If thermodynamic equilibrium exists, many flows can be exactly calculated and, in fact, are routinely analyzed in a number of common applications. When the flow permits continued chemical reactions, but is not in equilibrium, rate processes must be included and the calculation becomes much more difficult. In some of these cases, it is convenient to apply flow criteria which permit a comparison of the relative importance of chemical reaction times and characteristic dynamic flow times. The two extremes, i.e., either complete chemical equilibrium or completely frozen flow, can be viewed in the light of these typical times. When the chemical transformation processes are extremely rapid compared to the rate of change of gas flow parameters, chemical equilibrium can be expected. Conversely, if very large thermodynamic changes occur rapidly, the chemical kinetic rate processes may not be sufficiently fast to "keep up" and freezing of the chemical composition is probable. Flow criteria are available in some cases for predicting whether either of these conditions will prevail. Alternatively, predictions can be made in simplified flows for determining the location in an expanding flow where freezing will occur.

In the sections that follow, we examine a single typical reaction, follow its course through the sampling probe (whose non-reactive flow dynamics we have previously examined) and attempt to predict the state of the gases before they reach the very low pressure molecular-flow regime.

5.3.2 Chemical System and Near-Equilibrium Flow Criterion

Chlorine pentafluoride and hydrazine represent one of the highest performing, currently popular propellant systems actively being examined. The equilibrium composition of the combustion products of chlorine pentafluoride and hydrazine at a near-stoichiometric mixture ratio is given in Table VI. In this case and other examples of stoich and near-stoich mixtures at equilibrium, free atoms of H, F and Cl make up 15 to 20 percent (mole fraction) of the composition of the gases in the combustion chamber. As noted previously, these chamber products are cooled in the initial flow channel of the Rocketdyne/RPL sampling probe to approximately 1650°F and 166 psia.

Table VI

Equilibrium Composition of the Combustion Products of Chlorine Pentafluoride and Hydrazine at O/F = 3.1, 500 psia, 4084°K

Species	Mole Fraction
Cl	.090
HCl	.041
F	.055
HF	.602
H	.030
N_2	.173

We wish now to compare the time available for chemical changes in flowing through the probe with the time required for a given change. Inherent with relaxation effects is the coupling of separate chemical reactions; there are very few flow situations where a specific chemical reaction can be isolated to the exclusion of coupling effects. These effects might simply involve temperature changes with corresponding changes in reaction rates, or they could involve the formation of intermediates and different sets of reactions.

In an expanding gas with large reductions in temperature, the very fast two-body shuffling reactions merely exchange radical species, while the three-body recombination reactions are of greatest importance. Removal of radicals must be accomplished through the three-body reaction mechanism or by two active species colliding on a cooled wall, with the efficiency of the collision process connected to the nature of the third body. Since the transfer of vibrational energy to translational energy is essential to the stabilization of the newly combined species, a third body which can form a valence bond with either of the reactants should be more effective than an inert molecule. The composition indicated in Table VI should provide relatively efficient recombination.

For our present purpose for near stoichiometric mixture ratios, we will examine only the recombination of the dissociated hydrogen and fluorine in the cooling channel of the probe. If other independent reactions occur having characteristic reaction times of the same order of magnitude, the situation is similar to that of only a single reaction. For ox-rich mixtures, the three-body recombination of fluorine atoms would be the reaction of greatest interest to understanding probe behavior, while for fuel-rich mixtures, hydrogen atom recombination is important. Furthermore, since the chlorine is expected to behave similarly to fluorine, we take the combined concentrations of chlorine and fluorine to behave as fluorine alone. The chamber species assumed to enter the probe are therefore as indicated in Table VII. The third body required in the recombination collisions to remove the excess energy is shown as M and wall collisions are neglected. In Table VII, M is primarily HF and N_2, although other species are lumped into this value. Although the specific rate constant varies according to the nature of the third body, this difference is minor for present purposes. The concentrations and characteristic reaction times will be evaluated for the state of the gases at the channel entrance and exit. The reaction of present interest, then, is

$$H + F + M \underset{k_D}{\overset{k_R}{\rightleftharpoons}} HF + M$$

where k_R is the recombination rate constant and k_D the dissociation rate constant.

Table VII

Assumed Concentrations of Species Entering
Cooling Channel of Probe

Species	Mole Fraction	Concentration
F	.145	14.5×10^{-6} moles/cm^3
H	.030	3.00×10^{-6}
M	.825	82.5×10^{-6}

The two rate constants are related as usual by the equilibrium constant. The rate at which the concentration of hydrogen (H) changes is given by:

$$\left[\frac{\partial (H)}{\partial t}\right]_T = k_D (M) (HF) - k_R (H) (F) (M)$$

In an expansion with extremely rapid cooling, recombination reactions are much more prominent than the corresponding dissociative reactions. Therefore, the first term on the right side of the last equation can be neglected in comparison with the second term. With $k_D = 0$, the rate equation can be separated to give

$$\frac{d (H)}{(H)} = -k_R (F) (M)\, dt$$

By definition, this equation must be integrated at constant temperature which gives

$$\tau = \frac{\ln (H/H_o)}{-k_R (F)(M)}$$

τ in this case is the reaction time for the concentration to change from (H_o) to (H). In addition to the specified change in concentration, this reaction time is a function of the recombination rate constant and concentrations of other reactants. The rate constant to be used is an average value of the recombination constants recommended by Westenberg (14).

To calculate an upper limit to τ, we use the maximum gas temperature in the channel, the minimum species concentration (which both occur at the entrance) and arbitrarily permit a 10 percent change in hydrogen concentration. Then, for properties at the channel entrance,

$$\tau_{max} = \frac{-.106}{\frac{-8 \times 10^{18}}{4000}(14.5)(10^{-6})(82.5)(10^{-6})} = .044 \times 10^{-6} \text{ sec.}$$

Evaluated at channel exit conditions, $\tau \approx .01 \times 10^{-6}$ seconds

When these reaction times are compared to the total residence time of gases in the channel (14μ sec) there is little doubt that chemical equilibrium will be maintained.

Wegener (15) prefers not to make the above calculation but instead predicts departure from chemical equilibrium by a temperature lag, T'-T, which is a small positive number for expansions. In the case where T'-T is large, the flow has departed from equilibrium, however, no quantitative evaluation of the extent of departure is possible. Penner's near-equilibrium flow criterion (16,17) states that $T'-T=\tau(-dT/dt)$ where τ is the reaction time and -dT/dt is the cooling rate in the channel. The temperature lag for our simplified model is a maximum of $T'-T=(.044 \times 10^{-6})(3.4 \times 10^{8}) \approx 15^{\circ}K$. According to Penner (16), temperature lags less than $20^{\circ}K$ indicate that the flow is near-equilibrium. However as recommended in (15), the flow is in equilibrium only if the temperature lag is much smaller than the local temperature. This condition for equilibrium is arbitrarily specified as $(T'-T)/T \leq 10^{-3}$. In the present case, $(T'-T)/T \sim 4 \times 10^{-3}$ to 1×10^{-2} and is therefore marginally close to equilibrium at the channel entrance. Using calculated channel exit properties, $(T'-T)/T$ is less than 10^{-3} and the flow is near-equilibrium. This calculation does not correspond to the usual behavior in expanding nozzle flows where the gases are initially in equilibrium but the decreasing density results in abrupt freezing.

5.3.3 Frozen-Flow Criterion

When applied to a conventional nozzle expansion process, Bray's criterion (18) can be used to determine the location where the expanding gas composition freezes.* For all practical purposes, equilibrium is maintained to this point with frozen flow existing downstream. This rapid freezing is realistic because the characteristic chemical time for recombina-

* Although applied differently, Bray's criterion has been shown to be substantially equivalent to Penner's near-equilibrium flow criterion (19).

tion reactions is proportional to (density)$^{-2}$. Therefore, if density decreases as in a nozzle flow, the chemical time necessary to maintain equilibrium increases very rapidly. In the cooling channel of the probe, density does not change markedly.

The near-equilibrium criterion can only be used to predict the departure from equilibrium and not the extent of non-equilibrium. However, for flows without large composition changes, the near-frozen flow criterion can yield additional information. In the following, no attempt is made to fully describe the basis of the near-frozen flow criterion since this is done in (16). We will apply the available data in order to gain as much insight as possible into the characteristics of the RPL/Rocketdyne gas sampling probe.

Penner defines a reaction time,

$$\frac{1}{z} = k_R \rho^2 \left[\prod_{j=1}^{n} \left(\frac{Y_j}{W_j} \right)^{\nu' j} \right] \left[\sum_{i=1}^{n} (\nu_i'' - \nu_i')^2 \frac{W_i}{Y_i} \right]$$

which, when evaluated for the reaction and the constants used in the previous section for conditions at the channel entrance, yields the identical reaction time, $z = .044\,\mu$ seconds. In the above equation, all the notation is conventional (cf. 16).

The near-frozen flow criterion is given as:

$$\frac{Tc-T'}{Tc-T} \leq \left(-\frac{dT}{dt} \right)^{-1} \frac{1}{z} \left[1 - \frac{K_Y(Tc)}{K_Y(T)} \right] \left[- \left(\frac{d \ln K_Y}{dT} \right)_{Tc} \right]^{-1}$$

and if the left side is less than 10^{-2}, chemical reaction rates can be shown to have negligible effect on composition, i.e., the flow is frozen.

With the present probe, the following approximation holds;

$$\left(\frac{d \ln K_Y}{dT} \right) = \frac{\Delta Hc}{RTc^2} + \left[\frac{1}{p} \frac{dp}{dT} \right]_{Tc}$$

For typical atomic recombination reactions, $-\Delta Hc \approx 30$ kcal/mole and by graphically differentiating the pressure-temperature relationships at the probe entrance, we get $(d \ln K_Y/dT) \approx 10^{-3}\ ^oK^{-1}$. When $T \ll Tc$, $K_Y(T)/K_Y(Tc) \gg 1$ and $Tc-T'/Tc-T \approx 70$. The near-frozen flow criterion therefore also indicates that the gases in the cooling channel do not freeze, consistent with our previous conclusions.

It would be possible to apply again the near-equilibrium and near-frozen flow criteria in the region of the free-jet expansion downstream of the cooling channel if it were desirable to locate the precise region where freezing occurs.

Since the flow of chlorine pentafluoride/hydrazine products is in equilibrium, gas properties at the exit of the cooling channel can be calculated by routine procedures. Table VIII shows inlet and outlet compositions for a range of equivalence ratios. It can be seen that although free atoms compose roughly 15 percent of the chamber species, equilibrium conditions corresponding to the state of gases at the channel outlet permit almost no atoms but only diatomic molecules.

5.4 Free Jet Expansion

In the successive expansions experienced in the present RPL/Rocketdyne probe, the free jet formed at the outlet of the cooling channel is one of the most critical. The sample gases are still at relatively high temperature and pressure while the background gases are at approximately one atmosphere, a very high pressure for a sampling probe.

The flow from a highly underexpanded nozzle has a structure as sketched in Figure 17. Gases pass through the expansion fans, expand to the ambient pressure at the boundary and result in the shock structure indicated. In the case of only slightly underexpanded flow, the intercepting shocks meet at the centerline forming a repetitive diamond structure.

The details of free jet flow were first described by Owen and Thornhill (20) using a method of characteristics solution. They showed for an axisymmetric expansion that the flow inside an intercepting shock is isentropic and independent (or unaware) of the background until the Mach disc is reached.

A two-dimensional expansion, defined as the flow from a relatively long, narrow slit, provides more gradual gradients and a longer relative distance to accelerate to a given Mach number than the axisymmetric case. This can be seen in comparing the variations of Mach number with distance for the two-dimensional and three-dimensional expansions, given in Figure 18. Each of these solutions is valid only to the location of the first normal shock.

Table VIII

Approximate Species Concentrations at Cooling Channel Entrance and Exit for a Range of ClF_5/N_2H_4 Mixture Ratios

	O/F by weight	1.0	2.7	3.1	5.0
Cooling Channel Entrance	P_c (psia)	500	500	500	500
	T_c (°K)	2966	4057	4084	2828
	Mole Fraction				
	Cl	.0019	.0675	.0898	.1030
	ClF	-	.0001	.0002	.0337
	F	.0001	.0293	.0554	.2334
	F_2	-	-	-	.0004
	H	.0139	.0486	.0297	-
	H_2	.3293	.0262	.0089	-
	HCl	.0634	.0554	.0412	.0015
	HF	.3260	.5868	.6019	.4962
	N_2	.2655	.1857	.1728	.1244
Cooling Channel Exit	P_e (psia)	180	177	177	180
	T_e (°K)	1089	1200	1200	1089
	Mole Fraction				
	Cl	-	-	.0003	-
	ClF	-	-	-	.1829
	F	-	-	-	.0155
	F_2 (Cl_2)	-	-	(.0537)	.0558
	H	-	-	-	-
	H_2	.3375	.0021	-	-
	HCl	.0658	.1330	.0364	-
	HF	.3288	.6646	.7204	.5955
	N_2	.2675	.2004	.1892	.1474

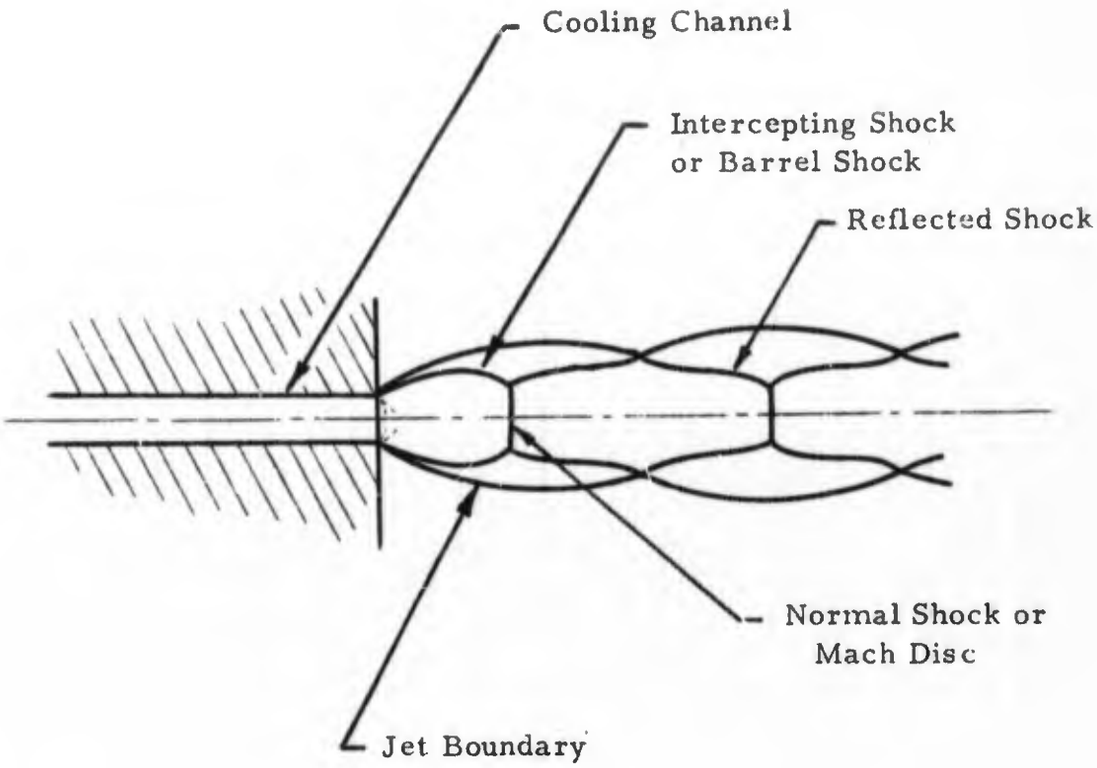

Figure 17

Sketch of Free Jet Structure for Highly Underexpanded Flow (Ref. 22)

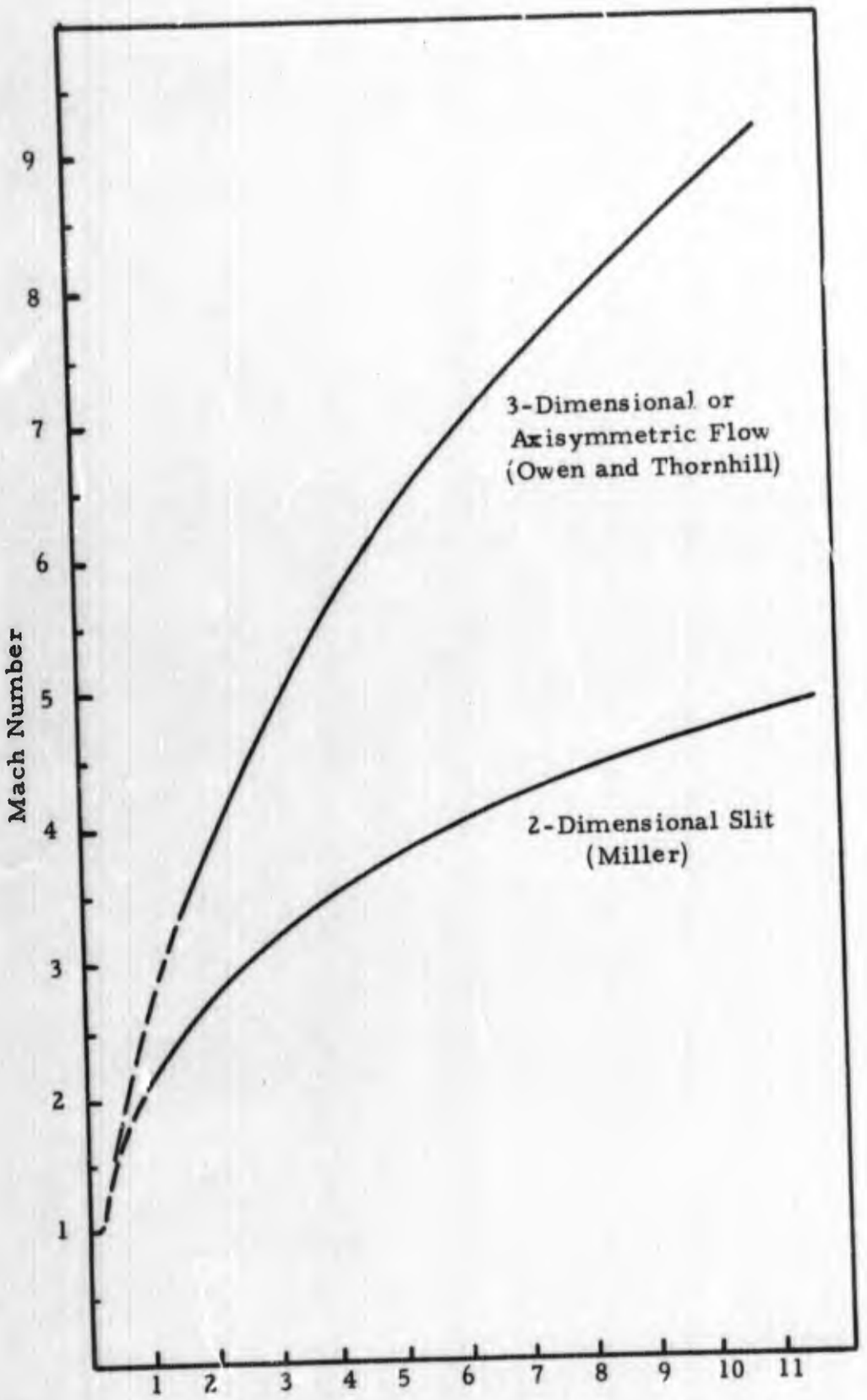

$$\frac{x_M}{D} = \frac{\text{distance from sonic surface}}{\text{characteristic dimension of flow port}}$$

Figure 18
Characteristic Solutions for Free Jet Expansion
With $\gamma = 1.4$ (Ref. 23)

Experiments have shown that for a highly underexpanded jet expanding into a static atmosphere, the location of the Mach disc is given by

$$\frac{x_M}{D} = .67\,(p_o/p_1)^{1/2}$$

for axisymmetric flows for all values of γ (21).

For chlorine pentafluoride-hydrazine products expanding in the cooling channel and flowing into a region of 14 psia, $x_M/D = .67 \times (287/14.0)^{1/2} = 3.04$. Adamson and Nicholls (22) prefer to locate the Mach disc by correlating with the static pressure at the nozzle exit. Using their experimental results, $x_M/D \approx 3.1$. For the axisymmetric case, therefore, with our pressure ratio, the Mach number just before the Mach disc is about 4.9.

Two-dimensional flows behave differently, however, and this type of jet structure has not been adequately defined. Since no experimental correlations exist, we must assume some specified gas behavior in the 2-D case. It seems reasonable to state that the Mach number variation on the centerline and the external shock structure will be similar in the 2-D and 3-D cases. We take the location of the Mach disc therefore to occur at the same Mach number in each case. This is consistent with theoretical and experimental results which show that the pressure downstream of the normal shock is approximately ambient, therefore, the Mach number at the entrance to this shock should be the same in either 2-D or 3-D geometry. From Figure 18, in the 2-D case, the Mach disc will be located at $x_M/D = 11.3$ corresponding to $M = 4.9$. Then, based on $D = .003$ in., which is the smaller dimension of the slit, the Mach disc is located at $x_M = .034$ inches.

After emerging from the normal shock, gases on the centerline are subsonic, but again accelerate and become supersonic. This wave pattern is repetitive (Figure 17) and theoretically duplicates itself. In reality, viscous effects become dominant and the structure rapidly dissipates. Generally, schlieren and direct photographs of exhaust plumes show 6 or 7 of the deteriorating wave patterns. Although the first section is slightly different than succeeding sections (24), if we assume all of them have the same wavelength, we see that the complete free jet emerging from the cooling channel will be greater than .40 inches in length. In the RPL/Rocketdyne probe, the distance from the cooling channel exit to the entrance of the first skimmer is .325 inches. The expanding free jet therefore goes through successive expansion cooling, shock reheating and ambient dilution for four or five cycles. After exposing the gas sample to this type of flow it is relatively unimportant whether an

additional bow shock exists at the entrance to the skimmer or whether the flow at the skimmer entrance is subsonic and no shock forms. It would not be possible to predict the exact flow field at the skimmer entrance in any event.

In an exhaust or free jet plume, background gases can be detected on the centerline as early as the second wavelength with increasingly larger amounts of dilution in succeeding wavelengths. With only inert gases in this chamber initially, dilution is relatively unimportant as combustion species first flow through the cooling channel. Only a small fraction of this flow goes through the skimmer, however, and the background quickly acquires high concentrations of colliding, reacting, wall-impinging combustion products. These products are then subsequently drawn through the skimmer (along with the appropriate products) and finally analyzed in the mass spectrometer.

There is another factor which should be considered in the gas behavior in this chamber. Data are available for axisymmetric flows to predict the shapes of free jets; in particular, maximum plume diameters are known in terms of other physical properties. Using the data given in (21), the maximum diameter of the barrel shock in terms of distance to the Mach disc, D_M/x_M, is 0.525 for $p_o/p_1 = 20$ and $\gamma = 9/7$. This merely states that the maximum barrel shock diameter is about one-half of the distance from the orifice to the Mach disc.

A 3-D approximation is easiest to apply and that will be done first, using the effective diameter D = .00545 in. Since $D_M/x_M = .525$, and $x_M/D = 3.1$ from consideration of the pressure ratios, $(D_M/x_M)x(x_M/D) = D_M/D = 1.63$. D_M therefore is approximately .009 in. Knowing the approximate location of the section of maximum width of the barrel shock, we can compare this with the space available for the free jet expansion to take place. For the 3-D approximation there appears to be no interference between the gas plume and the inner walls of the probe.

In the expansion from a slit (2-D), we saw that the distance to the Mach disc increased, that is, $x_M/D = 11.3$. Assuming that the section of maximum diameter is still defined by $D_M/x_M = .525$, then

$$\frac{x_M}{D} \times \frac{D_M}{x_M} = 11.3\,(.525) = \frac{D_M}{D} = 5.9$$

which states that the maximum barrel shock diameter is about 5.9 times the exit slit diameter. If we now take D to be the larger dimension of the slit,

.030 in., D_M is .178 in. The distance to the Mach disc, meanwhile, is $x_M = 11.3\,(.003) = .034$ in., since it is based on the smaller slit dimension. With these dimensions, the boundaries of the jet will definitely interfere with the probe walls.

It appears therefore that the conical gas expansion section shown in Figure 9 is not properly matched to the free jet expanding from the cooling channel.

5.5 Rarefied Gas Phenomena

5.5.1 Present Probe Considerations

After passing through the first chamber of the probe, which is maintained at about one atmosphere, sample gases encounter two skimmers separating chambers of lower pressure. Figure 19 is a sketch of the probe configuration giving relative locations and the nomenclature for the various components. Figure 19 is similar to Figure 8 described previously. Gaseous expansion from the cooling channel begins as a high density, collision-dominated flow. As collision rates decrease, the flow enters a transition region until far downstream, after passing through the skimmers, molecular collisions occur only rarely and the flow enters the molecular-flow regime. According to Hamel and Willis (25), free-jet flow will only approach a collision-free situation, never becoming completely free molecular. Thus, the region where a "last" collision occurs cannot be defined, although a location such as the middle of the transition region can.

To determine the behavior of gases in the second probe chamber, we apply some of the same principles described previously for the free jet expansion in the one-atmosphere chamber. If the flow at the entrance to the first skimmer is subsonic, the gases will reach Mach one at the exit of this orifice. Figure 18, for the axisymmetric case. Location of the disc is based on the pressure ratio and in this case is,

$$\frac{x_M}{D} = .67\,(po/pe)^{1/2} = .67\,(750/5 \times 10^{-3})^{1/2} = 260$$

Since D = .003 inches, the Mach disc would be located at .780 inches from the orifice, considerably behind the second skimmer placed at .375 inches.

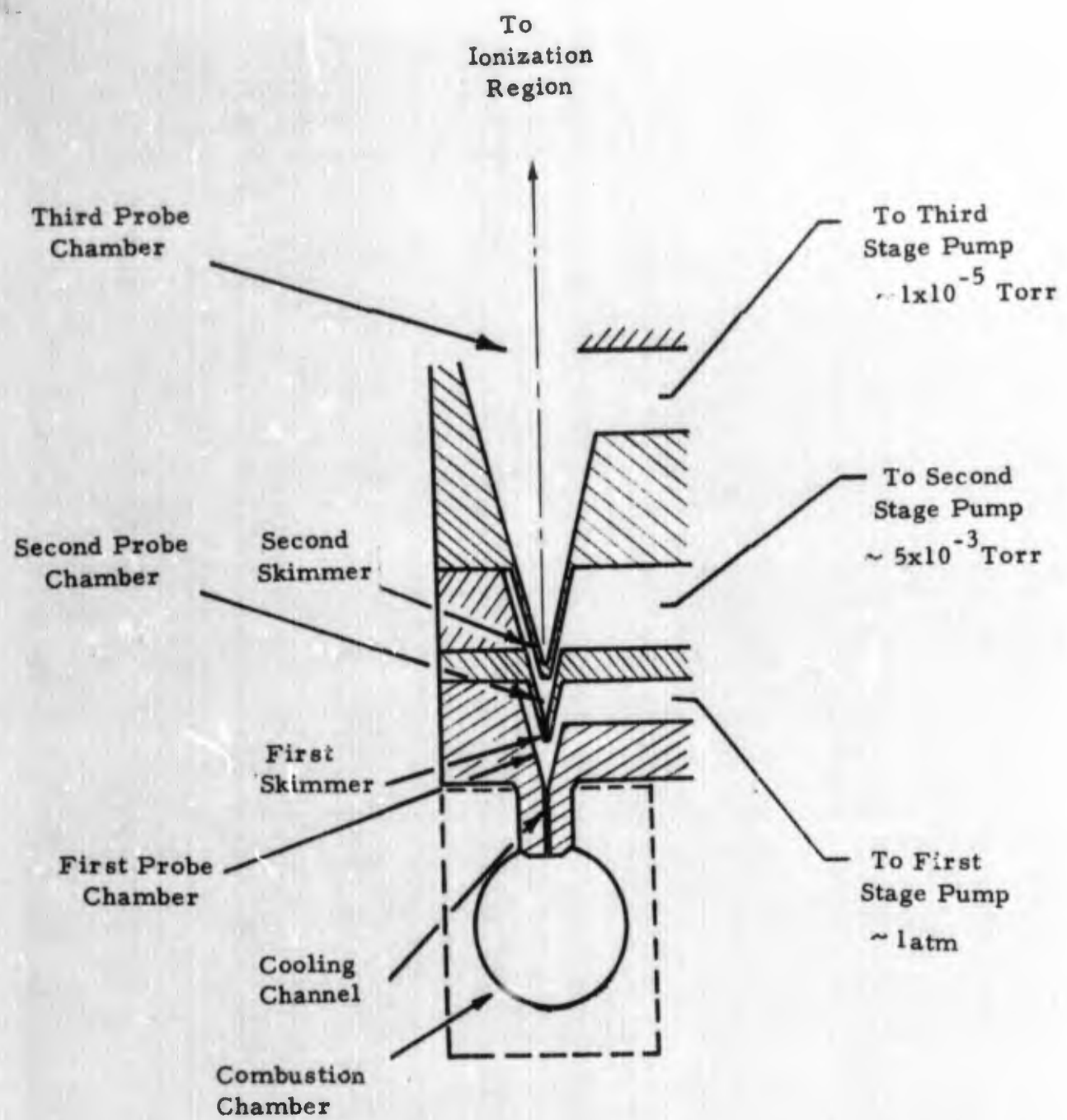

Figure 19

Schematic Diagram of Present RPL Sampling Probe
Attached to Combustion Chamber

If the continuum expansion could continue over the length of the second chamber, the Mach number at the entrance to the second skimmer would be given by (21)

$$M = A\left(\frac{x}{D}\right)^{\gamma-1} - \frac{1}{2}\left(\frac{\gamma+1}{\gamma-1}\right) \Big/ A\left(\frac{x}{D}\right)^{\gamma-1}$$

where the constant A = 3.96 for $\gamma = 9/7$. Evaluated at the entrance to the second skimmer, x/D = .375/.003 = 125 and $M \approx 12$.

The Mach number, however, is observed to level off as the gases leave the continuum regime and the expansion appears to "freeze". The terminal Mach number in this case is a function of Knudsen number based on nozzle diameter and stagnation mean free path (26) and is given as

$$M_T = 1.17\, K_{n_o} \exp\left[-(\gamma-1)/\gamma \right].$$

Based on gases leaving the first chamber at 14 psia, and entering the .003 inch skimmer at 1500°F with $\gamma = 1.2$, the Knudsen number (K_{n_o}) equals .0044 resulting in a calculated terminal Mach number of 2.79. If the flow is considered viscous and isentropic to this Mach number, gas temperature will be 640°F at this point. Since the transition from continuum to molecular flow occurs abruptly in a short axial distance, the frozen translational temperature will remain at this value. Equilibration of other molecular degrees of freedom must then be considered (23).

If we now assume that the gas temperature entering the skimmer is only 500°F (instead of 1500°F), the same procedure leads to a new conclusion. These two cases are summarized for $\gamma = 1.2$, $D_{orifice} = .003$ inches, po = 14 psia;

To (°F)	η (dynesec/cm²)	ρ (gm/in³)	c (ft/sec)	λ (in)	K_{n_o}	M_T	T Terminal °F
1500	411.6×10^{-6}	.0040	2250	13.3×10^{-6}	.0044	2.79	640
500	226×10^{-6}	.00825	1580	5.04×10^{-6}	.0017	3.25	8

We see that as inlet temperature is decreased, gas temperature at the freezing point also decreases but not quite as drastically. However, as the absolute temperature becomes lower, other considerations, such as condensation must be included.

5.5.2 Generalized Probe Requirements

Examination of the present probe design leads to the conclusion that the pressures existing at the manifold regions or at the inlets to the vacuum pumps (Figure19) probably do not indicate the true pressures existing in the regions of the molecular beam. This is due to the small conical passageways connecting these regions and their relatively poor low-pressure flow characteristics. Operation of the probe at RPL in a shock tube indicates that a cascading effect in pressurizing succeeding chambers occurs because of choking phenomena.

At this point in the description of the behavior of the present RPL/Rocketdyne probe, it is not worthwhile to continue to apply rarefied gas flow criteria to the specific conditions of use since the gases no longer are indicative of the true species existing in the combustion chamber and true operating conditions are uncertain. Therefore, examination of molecular beam formation and probe behavior from this point on should be generalized to permit a constructive examination of sampling requirements.

5.6 Mass Spectrometer Considerations

Successful detection of free radicals by mass spectrometer requires careful treatment of the radicals in traveling from the reactor to the ionization region of the masspec. The path of the inlet gas must be a straight line, preferably as short as possible. Naturally, as the pressure of the source of combustion species increases, greater pumping capacity, or a greater number of successive chambers and skimmers may be required.

The formation of a molecular beam is essential for a successful probe, to minimize transient times, to minimize wall collisions and to minimize continued reactions. As the sampled molecules enter the ionization chamber of the masspec, they are subjected to electron bombardment. No ionization takes place until the electrons are given sufficient energy. As this energy is increased, a parent molecular ion may be produced. With still more energetic electrons, polyatomic species will be dissociated into numerous positive ions. The problem in detecting free radicals in gases is to distinguish between (1) dissociative electron impact with a parent molecule capable of yielding the ion by the process

$$AB + e \longrightarrow A^{+} + B + 2e$$

and (2) the ionization of the free radical itself:

$$A + e \longrightarrow A^{+} + 2e.$$

Since the energy requirement of the first process exceeds the second by the dissociation energy of AB, the positive ion will appear sooner for the dissociated gas than for the undissociated species as the electron energy is increased.

In a sampling probe, it is desirable that as little alteration of the gas sample as possible takes place in order to permit the most reliable interpretation of the mass spectrum.

BLANK PAGE

6.0 AREAS OF POSSIBLE PROBE IMPROVEMENT

6.1 Variation of Cooling Channel Parameters

In the discussions of Section 5.2, conclusions were limited to the geometry and dimensions of the existing RPL/Rocketdyne probe. In this section, we wish to investigate areas of possible probe improvement. Initially, we would like to investigate improvements easily accomplished with the present components. The .003 x .030 x .375 inch long cooling channel results in a gas history, which, in the case of ClF_5/N_2H_4 combustion products, permits continued chemical reactions. Using the analysis described in Section 5.2.4, it is relatively easy to determine the effects of geometric variations of the present probe. In turn, if areas of possible improvement are indicated, these relatively minor changes could easily be incorporated into the present RPL/Rocketdyne probe.

The present probe cooling channel is a slot milled into a copper bar slit in halves. The bar is reassembled for insertion in the probe. Since this bar can easily be replaced, it is worthwhile to determine the effects of geometric changes which can readily be made.

Figure 20 shows how outlet gas temperature varies with equivalent diameter of the flow channel. Also indicated on the abscissa are some representative rectangular channel dimensions which will yield the equivalent diameters shown. Although outlet temperature reductions can be obtained by going to smaller cross-sectional channel dimensions, the order of magnitude improvements required to freeze reactions are not possible.

The effect of channel length for a given effective diameter is shown in Figure 21 To minimize wall collisions and recombinations, a short channel is desirable, however, we see that the outlet temperature of the gases increases very rapidly as the channel is shortened. Since channel flow is inherently poor for a sampling probe, temperature reductions through lengthening the channel may improve downstream difficulties but will ruin the integrity of the sample in the process.

The possibility of highly cooling the present probe, perhaps through the use of liquid nitrogen, is examined in Figure 22. For the present probe dimensions only minor gas temperature reductions are achieved, therefore this is not an effective route.

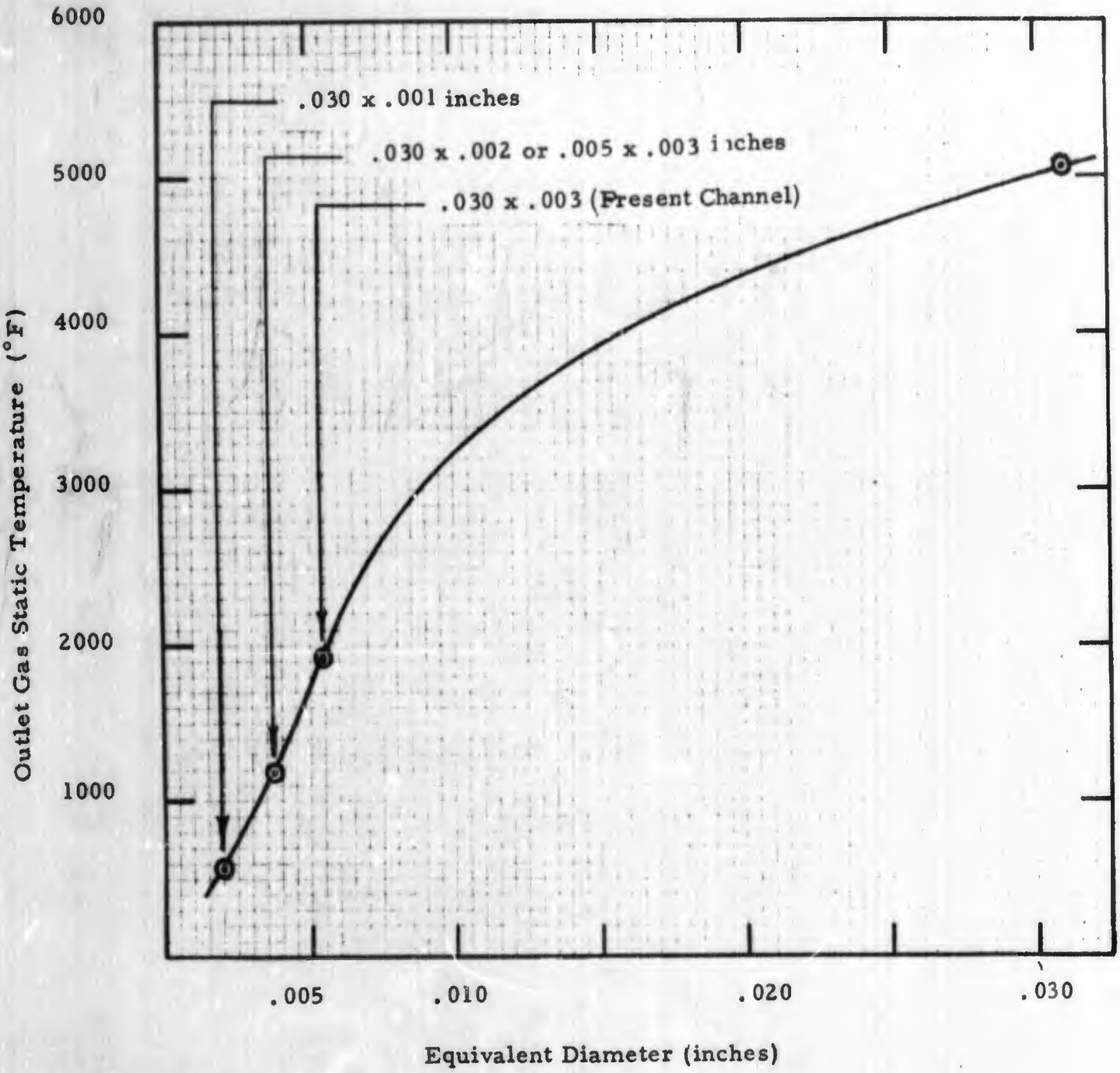

Figure 20

Influence of Probe Flow Diameter on Outlet Gas Temperature

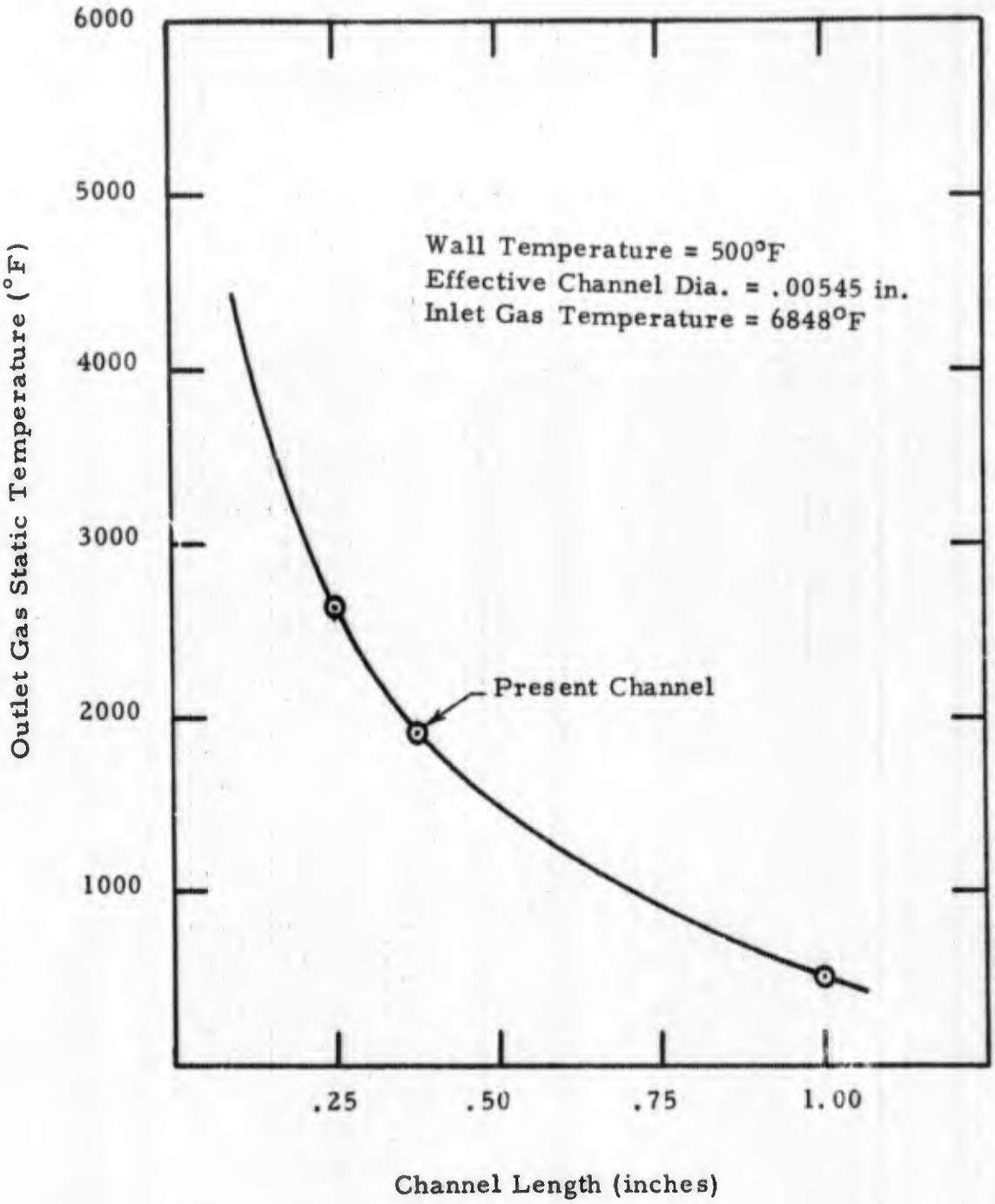

Figure 21

Influence of Probe Channel Length on Outlet Gas Temperature

Effective Diameter = 0.00545 in
Channel Length = .375 in
Outlet Gas Temperature = 6848 °F

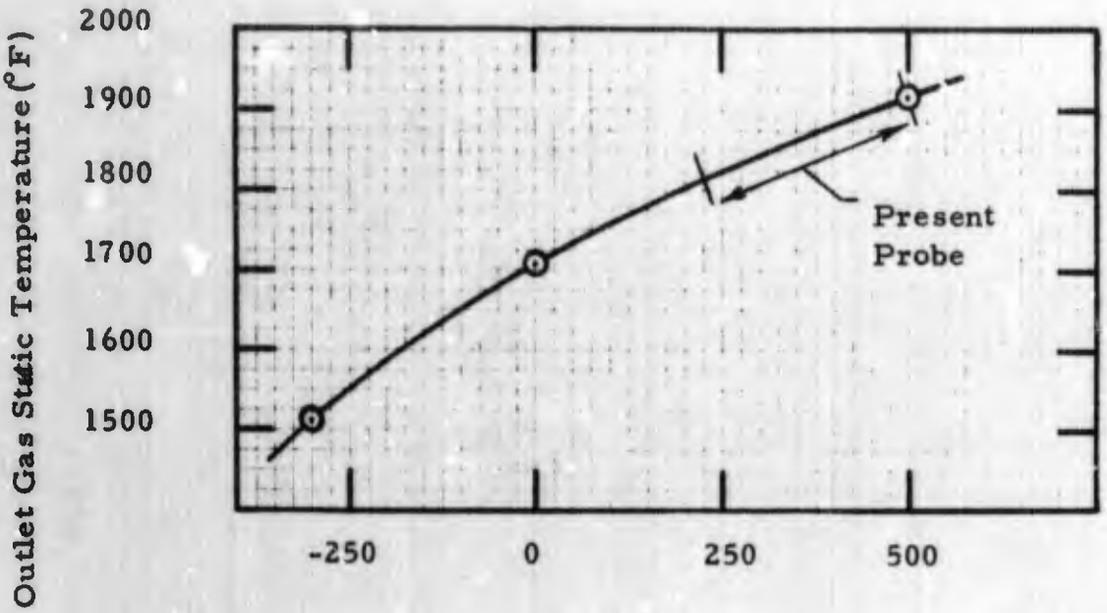

Figure 22

Influence of Probe Channel Wall Temperature on Outlet Gas Temperature

All of the data points used in the preceding graphs are summarized in Table IX. Outlet gas pressures are also shown. In addition, the effect of combustion chamber or channel inlet gas temperature on the outlet state from the present channel can be seen in the last calculation. Here, the inlet temperature is reduced to 90 percent of the theoretical value corresponding to c* ≈ 95 percent. A stagnation temperature reduction of 731°F at the inlet results in about a 270°F reduction in static temperature at the outlet of the channel.

It appears that minor changes in the present probe may improve the present situation but will not resolve basic shortcomings.

Table IX

Summary of Some Alternate Approaches to Using The Present KPL/Rocketdyne Probe

De (in)	L (in)	Tw (°F)	Tg (°F)	Outlet Temperature Static (°F)	Outlet Temperature Total (°F)	Outlet Pressure Static (psia)	Outlet Pressure Total (psia)
.031	.375	500	6848	5069	5960	254	457
.00545	↓	↓	↓	1917	2268	165	284
.00375	↓	↓	↓	1196	1478	137	236
.002	↓	↓	↓	570	799	111	185
.00545	.250	↓	↓	2632	3246	192	335
↓	1.00	↓	↓	508	722	109	179
↓	.375	-300	↓	1514	1890	152	277
↓	↓	0	↓	1710	2132	160	286
↓	↓	500	6117	1649	2090	166	287

6.2 Future Improvements

It is clear that the present RPL/Rocketdyne gas extraction probe is far from adequate. Not only is quantitative analysis of chamber species impossible, but qualitative results may also be misleading because many important chamber species, notably free radicals and atoms, will never enter the ionization region of the mass spectrometer.

The preceding section indicated that minor improvements are possible by keeping present probe components in the same basic assembly with slightly more cooling, slightly lower pressures in the first chamber and in general by doing everything slightly better than it is presently being done. After all these minor improvements are made, however, the comments of the top paragraph would still apply, though perhaps not quite as strongly. Thus, rather than taking the route of minimum change which cannot resolve basic shortcomings, we feel a significant change is necessary.

Because of the studies made in recent years in combustion research, gas sampling and rarefied gas dynamics, it appears that it is now possible to design a sampling system which truly may be effective. It is recommended that a water cooled orifice (which is as large as possible but sized in accordance with pumping capacity) is employed. A free jet expansion would be used which permits a skimmer to be placed upstream of the Mach disc. Preliminary consideration of pressure ratios and pumping requirements indicates that a first probe chamber pressure of about 1×10^{-3} mm Hg may be optimum. If initial probe chambers are designed for effective molecular beam formation, centerline gases will reach collision-free flow in a minimum time, will never suffer wall-collisions, will never encounter the reheating which accompanies flow through shocks, and will be affected least by background species. The problems associated with stagnating the high temperature gases at points downstream from the chamber remains to be determined.

Problems include optimizing the various probe chamber pressures and distances between orifices. In addition, if a probe is designed for sampling from 500 psia, it remains to determine whether performance will still be effective at 150 psia or other likely conditions of use.

7. CONCLUSIONS AND RECOMMENDATIONS

A unique laboratory combustor has been designed which permits the extraction of gas samples from any longitudinal position of the combustion chamber. Axial movement of the injector and exhaust nozzle within a stationary cylindrical barrel effectively moves the chamber past a fixed sampling port.

The combustor was fabricated and a demonstration test program was conducted. As a result of the successful completion of these efforts, it was concluded that the combustor design including the hot gas seal arrangement, method of actuation, cooling design and materials choices was satisfactory. The Movable Combustion Chamber is now available for use with a mass spectrometer in combustion studies. It is recommended that these studies be actively pursued with the existing chamber and other chambers.

The analysis of the present RPL gas sampling system (Phase III) indicated shortcomings in the existing design. The cooling channel is inherently poor since it permits recombination of active species. The free jet expansion at the exit of the cooling channel also behaves in a manner not desirable for a gas sampling system. Other factors contribute to the poor operation of the probe.

It is recommended that the sampling system be redesigned to provide an effective gas sampler capable of yielding quantitative analyses. It is believed that this is possible with a system not significantly different from the present system in overall size and use of vacuum pumping equipment.

8. REFERENCES

1. Kahrs, J., "Combustion Specie Sampling, Phase I- Design of a Movable Combustion Chamber", TCC-RMD Report 5530-I, November 1967.

2. Elverum, G. W. and Morey, T. F., "Criteria for Optimum Mixture-Ratio Distribution Using Several Types of Impinging-Stream Injector Elements", JPL-CIT Memorandum 30-5, Feb. 25, 1959.

3. Riebling, R. W., "Criteria for Optimum Propellant Mixing in Impinging-Jet Injection Elements", J. Spacecraft and Rockets, 4, No. 6, 817, June 1967.

4. Hill, P. R., "A Method of Computing the Transient Temperature of Thick Walls from Arbitrary Variation of Adiabatic-Wall Temperature and Heat-Transfer Coefficient", NACA Report 1372.

5. Summers, W. and McMullen, E. T., "Combustion of N_2H_4/N_2O_4 Propellant System", AIAA Paper 66-662, AIAA Second Prop. Spec. Conf. June 1966.

6. Sawyer, R. F., "Mass Spectroscopic Observation of Ignition Phenomena in a Small Rocket Combustion Chamber", WSCI -67-39.

7. Sawyer, R. R., McMullen, E. T. and Purgalis, P. "The Reaction of Hydrazine and Chlorine Pentafluoride in a Laboratory Rocket Combustor", AIAA Paper No. 68-92, AIAA 6th Aerospace Sciences Meeting, N. Y., Jan. 1968.

8. Rocketdyne Report AFRPL-TR-65-70, "Final Report, Development of a System for the Identification of Rocket Exhaust Products", April 1965.

9. Shapiro, A. H., The Dynamics and Thermodynamics of Compressible Fluid Flow , The Ronald Press, New York, 1953, Vols. I & II.

10. Brokaw, Richard S., "Alignment Charts for Transport Properties-Viscosity, Thermal Conductivity, and Diffusion Coefficients for Nonpolar Gases and Gas Mixtures at Low Density". NASA Technical Report TR R-81, 1961.

11. Svehla, Roger A., "Estimated Viscosities and Thermal Conductivities of Gases at High Temperature", NASA Technical Report TR R-132, 1962.

12. Eckert, E. R. G. and Drake, Robert M. Jr., Heat and Mass Transfer , New York: McGraw Hill Book Company, Inc. 1959.

13. McAdams, W.H., Heat Transmission, McGraw-Hill Book Co., New York, 1954.

14. Westenberg, A. A., and S. Favin, "Complex Chemical Kinetics in Supersonic Nozzle Flow", Ninth Symposium (International) on Combustion, 1962.

15. Wegener, P. P., "Experiments on the Departure From Chemical Equilibrium in a Supersonic Flow", ARS J., April 1960 p. 322. "Supersonic Nozzle Flow with a Reacting Gas Mixture", The Physics of Fluids 2, No. 3, May-June 1959, p. 264.

16. Penner, S. S., Chemistry Problems in Jet Propulsion, Pergamon Press, 1957.

17. Penner, S. S., "Near-Equilibrium Criteria for Complex Chemical Reactions during Flow Through a Nozzle", J. of Chemical Physics, 17, 841, 1949.

18. Bray, K.N.C. J. Fl. Mech. 6 part 1, July 1959, 1-32.

19. Penner, S. S., J. Porter and R. Kushida, "Rate and Radiative Processes During Flow in DeLaval Nozzles", Ninth Symposium (International) on Combustion, 1962.

20. Owen, P. L. and C. K. Thornhill, "The Flow in an Axially Symmetric Supersonic Jet From a Nearly Sonic Orifice into a Vacuum", Arm, Res. Est. Report No. 30/48.

21. Ashkenas, H. and F. Sherman, "Supersonic Free Jets - Structure and Utilization", in Rarefied Gas Dynamics, Fourth Symposium Supplement 3, Vol II, Academic Press, 1966.

22. Adamson, T. C. and J. A. Nicholls, "On the Structure of Jets From Highly Underexpanded Nozzles Into Still Air", J. of the Aeronautical Sciences, January 1959, 16.

23. Miller, D., "Rotational Relaxation of a Diatomic Molecule", Princeton University Ph. D Thesis, January 1966.

24. Love, E. S., C. E. Grigsby, Louise P. Lee, and Mildred J. Woodling, "Experimental and Theoretical Studies of Axisymmetric Free Jets", NASA TR R-6, 1959.

25. Hamel, B. B. and D. R. Willis, "Kinetic Theory of Source Flow Expansion with Application to the Free Jet", Phys. of Fluids, 9, No. 5, May 1966, 829.

26. Anderson, J. B., R. P. Andres, J. B. Fenn, and G. Maise, "Studies of Low Density Supersonic Jets" in Rarefied Gas Dynamics, Supplements, Vol II, Academic Press, 1966.

UNCLASSIFIED

Security Classification

DOCUMENT CONTROL DATA - R & D

(Security classification of title, body of abstract and indexing annotation must be entered when the overall report is classified)

1. ORIGINATING ACTIVITY (Corporate author)
Thiokol Chemical Corporation
Reaction Motors Division

2a. REPORT SECURITY CLASSIFICATION
Unclassified

2b. GROUP

3. REPORT TITLE
Combustion Species Sampling
Final Report

4. DESCRIPTIVE NOTES (Type of report and inclusive dates)
Final Report - 1 August 1967 - 1 May 1968

5. AUTHOR(S) (First name, middle initial, last name)
Jack Kahrs

6. REPORT DATE
June 1968

7a. TOTAL NO. OF PAGES
77

7b. NO. OF REFS
26

8a. CONTRACT OR GRANT NO.
F04611-68-c-0007

b. PROJECT NO.
Program Element No. 6.54.02.15.4

c.

d.

9a. ORIGINATOR'S REPORT NUMBER(S)
RMD 5530-F

9b. OTHER REPORT NO(S) (Any other numbers that may be assigned this report)
AFRPL-TR-68-120

10. DISTRIBUTION STATEMENT
Qualified requesters may obtain copies of this report from DDC

11. SUPPLEMENTARY NOTES

12. SPONSORING MILITARY ACTIVITY
Rocket Propulsion Laboratory
Edwards Air Force Base

13. ABSTRACT A combustion chamber for propellant studies was developed and molecular beam gas sampling systems were analyzed in this program. A unique laboratory combustor design provides sampling from any part of the chamber by axial movement of a gas extraction port while the engine operates at pressures up to 500 psia. Variable chamber volume is also possible during operation. Sealing of moving pistons is accomplished by metal piston rings and elastomeric o-rings. Hot firings of the combustor with chlorine pentafluoride and hydrazine were made to demonstrate the operation of all components. The most severe test was of sixty seconds duration at chamber pressure of 455 psia with adiabatic flame temperature in excess of 4000°K. Effective hardware cooling movement of the sampling station during firing and good combustion performance were successfully demonstrated. In another part of the program, an existing gas sampling probe was examined to determine its effectiveness in transferring combustion species to a mass spectrometer. A capillary quenching channel in the sampling probe cools combustion gases from 4000°K to 1200°K but allows all dissociated species (in the case of hydrazine/chlorine pentafluoride) to recombine. At the exit of this channel, an unconfined free jet forms a typical underexpanded exhaust plume and the combustion sample undergoes several successive cycles of expansion cooling, shock reheating and dilution by background gases. Skimmer locations and chamber pressures were examined for suitable molecular beam formation. Recommendations are given for the design of more effective sampling probes.

DD FORM 1 NOV 68 1473

UNCLASSIFIED

Security Classification

14. KEY WORDS	LINK A		LINK B		LINK C	
	ROLE	WT	ROLE	WT	ROLE	WT
Combustion Species Sampling						
Sampling Probe						
Gas Analysis						
Laboratory Combustor						
Free Jet Expansion						
Rarefied Gases						
Molecular Beams						
Mass Spectrometer						